THE JOURNAL OF BIOLOGICAL CHEMISTRY
Vol. 280, No. 7, Issue of February 18, pp. 6181–6196, 2005
Printed in U.S.A.

Estrogen-induced Spermatogenic Cell Apoptosis Occurs via the Mitochondrial Pathway

ROLE OF SUPEROXIDE AND NITRIC OXIDE*

Received for publication, May 28, 2004, and in revised form, November 8, 2004
Published, JBC Papers in Press, November 15, 2004, DOI 10.1074/jbc.M405970200

Durga Prasad Mishra and Chandrima Shaha‡

From the National Institute of Immunology, Aruna Asaf Ali Marg, New Delhi 110067, India

The detrimental effects of estrogen on testicular function provide a conceptual basis to examine the speculative link between increased exposure to estrogens and spermatogenic cell death. Using an *in vitro* model, we provide an understanding of the events leading to estrogen-induced apoptosis in cells of spermatogenic lineage. Early events associated with estrogen exposure were up-regulation of FasL and increased generation of H_2O_2, superoxide, and nitric oxide. The ability of anti-FasL antibodies to prevent several downstream biochemical changes and cell death induced by 17β-estradiol substantiates the involvement of the cell death receptor pathway. Evidence for the amplification of the death-inducing signals through mitochondria was obtained from the transient mitochondrial hyperpolarization observed after estradiol exposure resulting in cytochrome *c* release. A combination of nitric oxide and superoxide but not H_2O_2 was responsible for the mitochondrial hyperpolarization. Mn(III) tetrakis(4-benzoic acid)porphyrin chloride, an intracellular peroxynitrite scavenger, was able to reduce mitochondrial hyperpolarization and cell death. Although nitric oxide augmentation occurred through an increase in the expression of inducible nitric-oxide synthase, superoxide up-regulation was a product of estradiol metabolism. All of the above changes were mediated through an estrogen receptor-based mechanism because tamoxifen, the estrogen receptor modulator, was able to rescue the cells from estrogen-induced alterations. This study establishes the importance of the independent capability of cells of the spermatogenic lineage to respond to estrogens and most importantly suggests that low dose estrogens can potentially cause severe spermatogenic cellular dysfunction leading to impaired fertility even without interference of the hypothalamo-hypophyseal axis.

The significance of estrogen effects on the male reproductive system is of great interest because of the demonstration of impaired fertility in mice lacking estrogen receptor-α (1, 2) and the discovery of a second estrogen receptor-β (3, 4), which is expressed in most of the cells of spermatogenic lineage (5). Another important reason for the increased attention on the role of estrogens in male reproduction stems from various reports of estrogen exposure in the environment having a detrimental effect on male reproductive development and health (6, 7). Because estrogen receptors are present on spermatogenic cells, agents able to mimic the hormone can potentially bind to its receptor, leading to functional impairment of the male gamete. This hypothesis is validated by reports of lowered fertility rates in wildlife populations as a consequence of exposure to agents with estrogenic activity, termed endocrine disruptors (8, 9). In addition, observations suggest that exposure to estrogens and estrogen-like chemicals interferes with testicular steroidogenesis (10), and neonatal exposure ensures disturbances of puberty onset (11). Bisphenol A, considered an environmental estrogen, exerts detrimental effects on mouse testis (12), creates interference with rat testicular steroidogenesis (13), and induces Sertoli cell apoptosis in culture (14). As evident from the above studies, the effect of estrogen on spermatogenesis is amply indicated in the literature; however, the understanding of a direct action of the hormone on spermatogenic cells is virtually nonexistent. This is because estrogen administration *in vivo* interferes with the hypothalamo-pituitary axis, and observed changes would be the result of testosterone deprivation rather than a direct effect of estrogen on the spermatogenic cells. Taken together, the effect of estrogens on testicular function provides a conceptual basis to examine the speculative link between increased exposure to environmental estrogens and reduced fertility.

Estrogens act primarily through nuclear estrogen receptors, where binding of hormone and receptor brings about conformational changes, thus enabling the estrogen to recruit transcriptional coactivators that regulate gene expression leading to the control of a variety of functions (5). Effects of estrogens vary for different cell types ranging from induction of cell proliferation (15) to initiation of apoptosis (16–19). Apoptosis is of great relevance for successful production of spermatogenic cells because excess cells need to be removed for the proper maintenance of testicular homeostasis (20). Selection of the apoptotic pathway depends on the physiological and pathological state of the cells. Members of the Bcl-2 family of proteins and Fas-FasL system have been implicated in spermatogenic cell apoptosis under various conditions (20, 21). Although earlier studies implicated FasL of Sertoli cell source for engaging Fas receptors on spermatogenic cells for apoptosis induction (21), later studies provided evidence in support of both Fas and FasL being expressed in spermatogenic cells as well (22, 23), thereby raising the possibility that FasL of spermatogenic cell source might be the ligand for Fas expressed on the various cell types of spermatogenic origin. Up-regulation of Fas and FasL in response to estrogens in adult rat testis resulting in the apoptosis of spermatogenic cells was shown in an earlier report from this laboratory, but the consequences of any direct estrogen action on spermatogenic cells could not be deciphered from this investigation (22).

* This work was supported by grants to the National Institute of Immunology from the Department of Biotechnology and a grant from the Indo-United States Collaboration on Contraceptive and Reproductive Health Research. The costs of publication of this article were defrayed in part by the payment of page charges. This article must therefore be hereby marked "*advertisement*" in accordance with 18 U.S.C. Section 1734 solely to indicate this fact.

‡ To whom correspondence should be addressed. Tel.: 11-26703627; Fax: 11-26162125; E-mail: cshaha@nii.res.in.

The relationship between estrogen and FasL is not clear. In the normal ovary, FasL expression increases during high estrogen periods (24), whereas thymic atrophy resulting from estrogen treatment occurs via an increase in FasL expression (25) thereby indicating a relationship between increased FasL and estrogen. It is believed that the Fas-FasL system is responsible for maintaining the proper cell number in the testis during spermatogenesis (26), but the role of estrogen in Fas-FasL regulation during normal spermatogenesis is not known. Estrogens show diverse effects on cells, and there is an intimate relationship between them and reactive oxygen species (ROS).[1] The hormones are able to generate ROS through redox cycling of their semiquinone derivatives (27), and these ROS can cause considerable damage to cells (28). Fas-FasL ligation is also capable of generating ROS, and this ROS production occurs prior to caspase-8 activation in B cell lymphomas (29) and monocytes (30). On the other hand, in murine intestinal epithelial and PC12 cells oxidative stress is able to induce expression of Fas-FasL (31). It is not known whether ROS is generated in spermatogenic cells in response to estrogens or whether there is any interplay between Fas-FasL ligation and ROS. Data on responses of spermatogenic cells to estrogens are scanty, and the relationship between the various changes that estrogen receptor-ligand interaction would incur in these cells and the functional consequences need to be explored.

The present study was designed to investigate (i) the early changes that occur as a result of a direct estrogen action on the cells of spermatogenic lineage and (ii) the functional consequences of such changes. We provide an understanding of the critical events that occur after estradiol exposure to spermatogenic cells which lead to the activation of both the extrinsic and the intrinsic pathways of apoptosis.

EXPERIMENTAL PROCEDURES

Materials—The Apoptosis Detection System was procured from Promega (Madison, WI). Primary and secondary antibodies were from Santa Cruz Biotechnology Inc. (Santa Cruz, CA) and Jackson Immunoresearch (West Grove, PA). For color development, a Vector Immuno Peroxidase substrate kit for Western blots was procured from Vector Laboratories Inc. (Burlingame, CA). AmpliTaq Gold reverse transcriptase was from Roche Applied Science. JC-1, CM-H_2DCFDA, DAF-FM, the Vybrant apoptosis assay kit, the Griess reagent kit, the Enz-Check® caspase-3 assay kit, and SNAP were obtained from Molecular Probes (Eugene, OR). TRIzol reagent was from Invitrogen. MnTBAP was obtained from Calbiochem (La Jolla, CA). Caspase-8 inhibitor, Z-Leu-Glu-Thr-Asp-FMK (Z-LETD-FMK) was purchased from MP Biomedicals Inc. (Aurora, OH). Tamoxifen and all other chemicals were purchased from Sigma.

Animals—Adult male Wistar rats (*Rattus rattus*) were obtained from the Small Animal Facility of the National Institute of Immunology, New Delhi. Wild type C57BL/6 (B6) and B6.MRL.lpr (B6-lpr,lpr) mice were obtained from Jackson Laboratory (Bar Harbor, ME) and maintained at the Small Animal Facility of the National Institute of Immunology following standards specified by the Institutional Animal Ethics Committee (IAEC) of the National Institute of Immunology, New Delhi. Euthanasia of rats was carried out by CO_2 inhalation as specified by the IAEC, and testes were collected for the preparation of spermatogenic cells.

Treatments—Spermatogenic cells cultures in Ham's F-12 medium and Dulbecco's modified Eagle's medium, supplemented with 14.2 mM sodium bicarbonate, 10 mM sodium pyruvate, 2 mM L-glutamine, 1 mM sodium pyruvate, 10^{-7} M testosterone, and 1% bovine serum albumin were treated with 10^{-8} M 17β-estradiol. The dilutions of 17β-estradiol were made in sterile double distilled water because this estradiol was water-soluble (Sigma). Tamoxifen was dissolved in ethanol, and dilutions were made in culture media at the time of experimentation to arrive at a dose of 10 nM. *N*-Acetylcysteine (NAC), an antioxidant, was dissolved in culture medium, and the pH was adjusted to 7.0. NAC was used at a concentration of 20 μM, and cells were either preincubated with NAC prior to 17β-estradiol exposure, or NAC was added at different time points after initiation of 17β-estradiol treatment. Aminoguanidine (AG), the inducible nitric-oxide synthase (iNOS) inhibitor, was dissolved in sterile double distilled water and used at a concentration of 50 μM. It was either added 2 h prior to the addition of 17β-estradiol or added again at 4 h after 17β-estradiol exposure was initiated. MnTBAP (dissolved in sterile double distilled water) was used as a scavenger of peroxynitrite at a dosage of 100 μM. To generate superoxide, cells were placed in medium containing 50 μM xanthine, and 0.05 μM xanthine oxidase prepared in culture medium was added to start superoxide generation. For production of nitric oxide (NO), SNAP dissolved in dimethyl sulfoxide was added to the cell suspension at a dosage of 4 μM. For all additions controls received equal amounts of vehicle.

Preparation of Cells—Spermatogenic cells were prepared according to Meistrich *et al.* (32) with slight modifications as described previously (22, 33). Briefly, decapsulated rat testes were finely chopped in spermatogenic cell culture medium, and the cells were subjected to serial filtration through nitex mesh (1,000 and 20 μm), Mira cloth, and glass wool. The resultant suspension was centrifuged and resuspended, and flow cytometry was used to check the cell preparation as described earlier (22, 33).

Preparation of Cytosol—Briefly, 10^8 spermatogenic cells were suspended in a buffer containing 150 mM sucrose, 10 mM succinate, 5 mM potassium phosphate, 10 mM HEPES-KOH, pH 7.4, and 0.1% bovine serum albumin in the presence of a mixture of protease inhibitors (1.6 mg/ml benzamidine HCl, 1 mg/ml phenanthroline, 1 mg/ml aprotinin, 1 mg/ml leupeptin, 100 mM phenylmethylsulfonyl fluoride) and lysed by nitrogen cavitation (450 pounds/square inch for 30 min at 4 °C) with constant stirring. The lysate was centrifuged sequentially at 500 and 2,500 $\times$ *g* for 10 min at 4 °C to remove unbroken cells and nuclei, respectively. The supernatant obtained was centrifuged at 100,000 $\times$ *g* for 1 h at 4 °C in a Optima XL-100K ultracentrifuge (Beckman) to obtain cell cytosol.

Reverse Transcription-PCR for FasL—Reverse transcription-PCR was carried out as described previously (22). Briefly, total RNA was isolated from spermatogenic cells after completion of various treatments using TRIzol reagent. First strand complementary DNA was made using 1–5 μg of total RNA in the presence of AmpliTaq Gold reverse transcriptase and random primer. After the reverse transcription, 1 μl of incubation mixture was used as a template for the subsequent PCR. Primer sets used as a template to obtain PCR products of FasL were 5′-AGCCCGTGAATTACCCATGTC-3′ and 5′-TGCTGGGGTTGGCTATTTGCT-3′ and for β-actin were 5′-AGGCATCCTGACCCTGAAGTAC-3′ and 5′-TCTTCATGAGGTAGTCTGTCAG-3′. All PCRs were performed for 30 cycles with an annealing temperature of 55–65 °C in 1.5 mM $MgCl_2$.

TUNEL Staining—Terminal deoxynucleotidyltransferase enzyme (TdT)-mediated dUTP nick end labeling (TUNEL) to detect DNA fragmentation was carried out using a TUNEL assay kit according to the manufacturer's instructions and as described previously (33). Briefly, cells were fixed in 4% formaldehyde, and postfixation permeabilization was carried out with 0.2% (v/v) Triton X-100 for 10 min at room temperature followed by incubation with buffer containing nucleotide mix (50 μM fluorescein-12-dUTP, 100 μM dATP, 10 mM Tris-HCl, pH 8.0, 1 mM EDTA, pH 7.6) for 1 h at 37 °C. TdT labeling was either measured by flow cytometry or visualized by microscopy.

Visualization of Phosphatidylserine Exposure—Annexin-V labeling was performed as per the manufacturer's instructions using a Vybrant apoptosis assay kit. Briefly, cells after the respective treatments were washed with ice-cold phosphate buffer and suspended in annexin-V binding buffer (50 mM HEPES, 700 mM NaCl, 12.5 mM $CaCl_2$, pH 7.4) and incubated for 15 min with annexin-V conjugated to Alexa Fluor and 10 μg/ml propidium iodide (PI). Subsequently, cells were washed and resuspended in the same buffer.

Microscopy—All samples for microscopy were analyzed with a Nikon Confocal microscope C1 using argon laser (488 nm) for green fluorescence of annexin-Alexa Fluor, DAF-FM and H_2DCFDA. For red and blue dyes, a red HeNe laser (543 nm) and a blue-diode laser (408 nm),

[1] The abbreviations used are: ROS, reactive oxygen species; AG, aminoguanidine; CM-H_2DCFDA, (5- (and 6-)chloromethyl-2′,7′-dichlorodihydrofluorescein diacetate); DAF-FM, 4-amino-5-methylamino-2′,7′-difluorofluorescein diacetate; $\Delta\psi_m$, mitochondrial membrane potential; E2, estradiol; FITC, fluorescein isothiocyanate; FIU, fluorescence intensity units; iNOS, inducible nitric-oxide synthase; JC-1, (5,5′,6,6′-tetrachloro-1,1′,3,3′-tetraethylbenzimidazolylcarbocyanine iodide); MnTBAP, Mn(III) tetrakis(4-benzoic acid)porphyrin chloride; NAC, *N*-acetylcysteine; NO, nitric oxide; PI, propidium iodide; SNAP, *S*-nitroso-*N*-acetylpenicillamine; TUNEL, terminal deoxynucleotidyltransferase enzyme (TdT)-mediated dUTP nick end labeling; Z-LETD-FMK, benzyloxycarbonyl-Leu-Glu-Thr-Asp-fluoromethyl ketone.

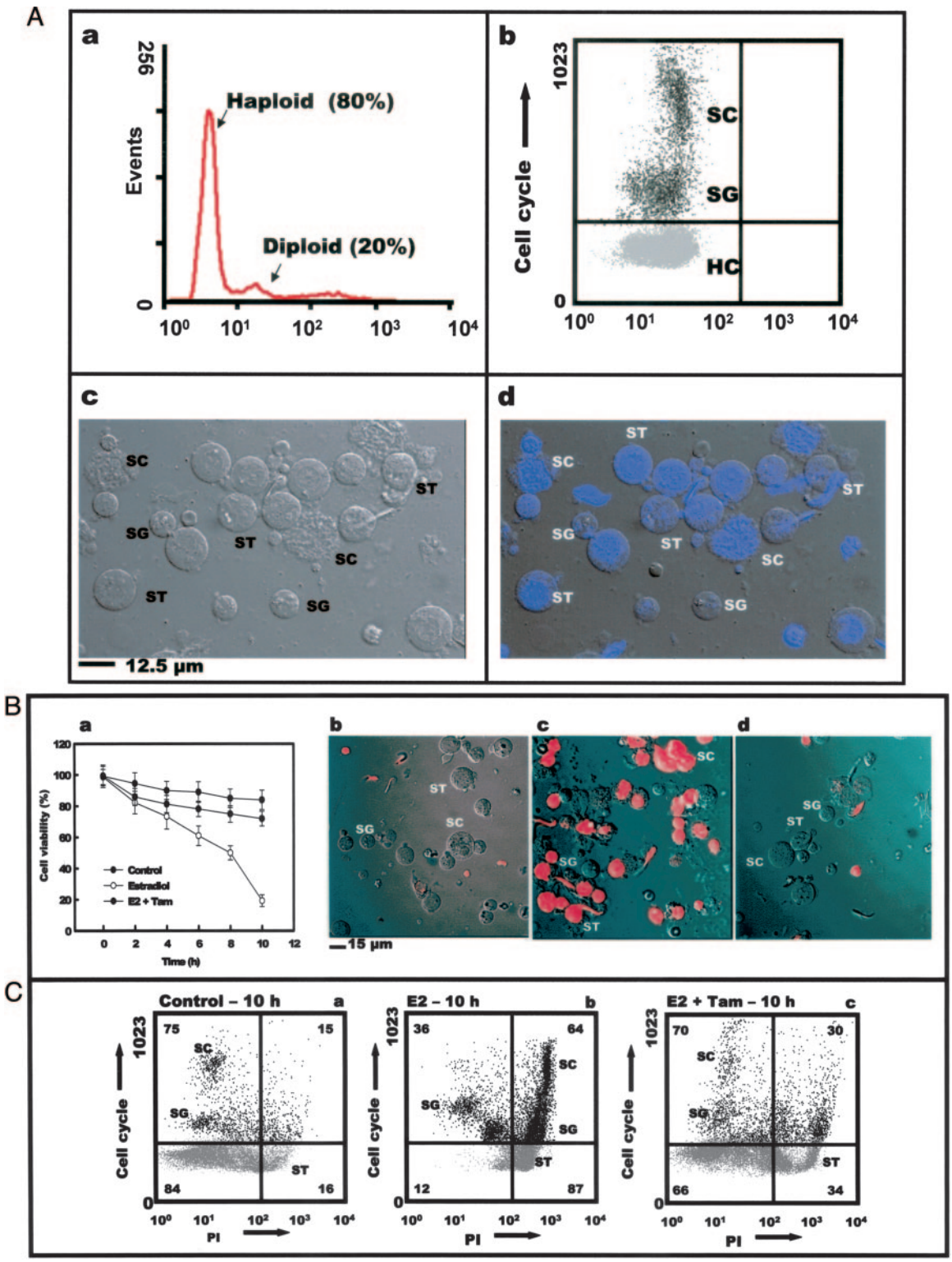

FIG. 1. **17β-Estradiol induces spermatogenic cell death *in vitro*.** *A*, profile of cell preparation. *a*, flow cytometric analysis of the spermatogenic cell preparation showing the predominant cell types present. Note that 80% haploid cells and 20% diploid cells were recovered. *b*, dot plot showing the prevalence of different cell types. The *y* axis represents cell separation based on DNA content. Meiotic cells, the primary spermatocytes (*SC*) with 4C DNA in the *upper quadrant* are followed by spermatogonia (*SG*) with 2C DNA and the postmeiotic haploid cells (*HC*) with 1C DNA in the *lower quadrant*. *c*, Nomarski photomicrograph of the cell preparation showing the cell types present. *d*, Hoechst staining of the same preparation clearly showing the diffused chromatin of the spermatocytes and the condensed nuclei of the spermatid. *ST*, spermatids. *B*, cell viability after 17β-estradiol treatment. *a*, percentages of total cell death in response to estradiol over a period of 10 h. Note the increase in cell survival when 10 nM tamoxifen (*Tam*) was present during estradiol treatment. *b–d*, Nomarski photomicrographs overlapped with PI staining in confocal recordings of cells treated with estradiol for 10 h. *b*, control; *c*, estradiol treatment; *d*, estradiol treatment in the presence of tamoxifen. *C*, analysis of cell death in dot plots. The *y* axis represents cell separation based on DNA content, and the *x* axis represents PI staining in a log scale with shifts representing increase in staining. The *numbers* in each *quadrant* represent the percentages of cells. The *upper two quadrants* represent total diploid cells, and the *lower two quadrants* represent total haploid cells. *a*, control at 10 h showing 84% haploid and 75% diploid cells negative for PI. *b*, estradiol treatment at 10 h showing a major shift in PI staining with 64% of diploid and 87% of haploid cells positive for PI. *c*, dot plot of cells treated with estradiol in the presence of 10 nM tamoxifen at 10 h. Note the reduction in the number of PI-positive cells. Data are representative of three experiments.

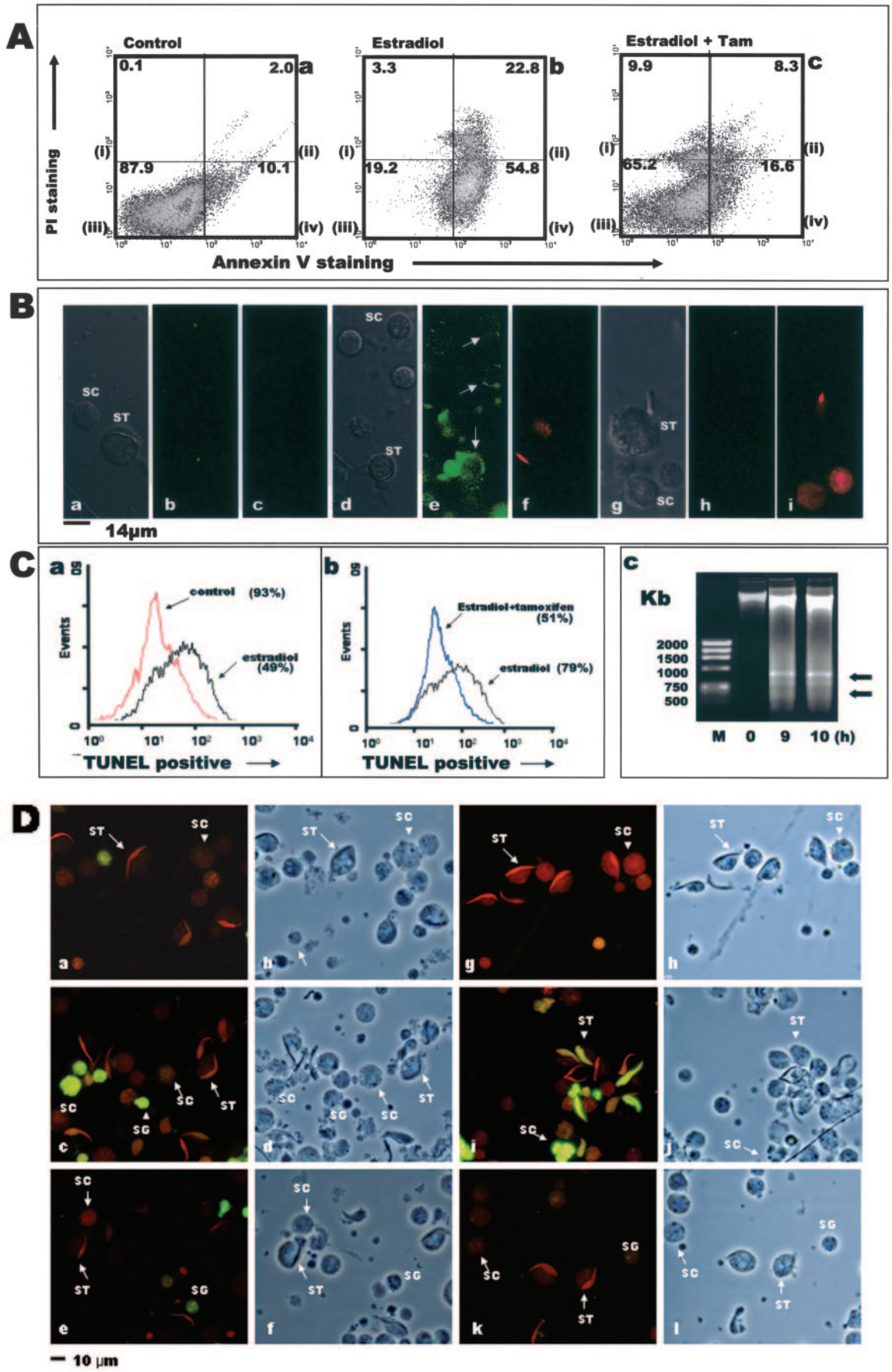

FIG. 2. **17β-Estradiol treatment results in phosphatidylserine exposure and DNA fragmentation.** *A* and *B*, phosphatidylserine exposure. Annexin-V binding and PI uptake of spermatogenic cells at 8 h after 17β-estradiol exposure are shown. Results shown are representative of three experiments, and 50,000 cells were analyzed in each case. *Numbers* within the *quadrant* represent the percentages of cells. The *quadrants*

respectively, were used for scanning PI and Hoechst-stained samples. Nomarski images were recorded in the transmission mode.

Flow Cytometry—Cells (10^6) from different experimental groups were run on an EPICS Elite ESP flow cytometer (Beckman Coulter, Fullerton, CA) equipped with a 15-mV, 488-nm air-cooled argon ion laser and 325-nm HeCd laser. The optimized instrument parameters were as follows: for forward scatter, voltage 100 mV, gain 30; for side scatter, voltage 400 mV, gain 30; for fluorescence 1 (Alexa Fluor/FITC), voltage 500 mV, mode log; fluorescence 3 (PI), voltage 550 mV, mode log; fluorescence 5 (Hoechst), voltage 560 mV, mode linear. Cells were isolated from fragments by gating on the forward and side scatter signals, and then cells were detected and analyzed according to their relative fluorescence intensities compared with unstained cells. Analyses were performed on 100,000 gated events, and numeric data were processed using WinMDI shareware version 2.8.

Nitrite Estimation—Nitrite estimation was carried out using a Griess reagent kit. Briefly, supernatants of spermatogenic cell culture for various treatment groups were collected at different time points and mixed with Griess reagent and incubated at room temperature. Nitrite standard solutions were prepared as per the manufacturer's protocol and mixed with Griess reagent. Absorbance was measured at 548 nm in a microplate reader (μ-quant, Biotek Instruments). Nitrite concentrations (nmol/10^6 cells) were calculated from the standard curve.

Measurement of Mitochondrial Membrane Potential—Mitochondrial membrane potential ($\Delta\psi_m$) was measured using JC-1 probe (34). JC-1 is a cationic mitochondrial vital dye that is lipophilic and becomes concentrated in the mitochondria in proportion to the membrane potential; more dye accumulates in mitochondria with greater $\Delta\psi_m$ and ATP generating capacity. Therefore, the fluorescence of JC-1 can be considered as an indicator of relative mitochondrial energy state. The dye exists as a monomer at low concentrations (emission, 530 nm, green fluorescence) but at higher concentrations forms J-aggregates (emission, 590 nm, red fluorescence). Briefly, cells were labeled for 10 min with 10 μM JC-1 at 37 °C, washed, resuspended in medium, and fluorescence was recorded at two different wavelengths as mentioned above. The ratio of the reading at 590 nm to the reading at 530 nm (590:530 ratio) was considered as the relative $\Delta\psi_m$ value.

Measurement of ROS—For measurement of H_2O_2, the cell permeant probe CM-H_2DCFDA was used. Although it detects hydroxyl radical, the half-life of the radical being short means that the primary detection is that of H_2O_2 (35). CM-H_2DCFDA is a nonpolar compound that readily diffuses into cells, where it is hydrolyzed to the nonfluorescent derivative dichlorodihydrofluorescein and trapped within the cells. In the presence of a proper oxidant, dichlorodihydrofluorescein is oxidized to the highly fluorescent 2,7-dichlorofluorescein. The dye was dissolved in dimethyl sulfoxide, and dilutions were made in culture medium. Briefly, cells (10^7) were suspended in medium containing 2 μg/ml CM-H_2DCFDA for 15 min in the dark, and various treatments were initiated. Fluorescence was monitored at an excitation wavelength of 488 nm and an emission wavelength of 530 nm over a period of time. For superoxide anion detection, OxyBURST reagent was used following the protocol described by the manufacturer. Briefly, cells (10^7) were loaded with OxyBURST Green H_2HFF-bovine serum albumin (10 μg/ml) at 37 °C for 2 min, and relative fluorescence was monitored for OxyBURST at an excitation wavelength of 488 nm and emission wavelength of 520 nm over a period of time. For NO, typically, 10^7 cells were loaded with 1 μM fluorescence probe DAF-FM for 30 min, washed, and treatments were initiated after which NO generation was monitored at an excitation of 485 nm and emission at 515 nm. For each experiment, fluorometric measurements were performed in triplicate and expressed as fluorescence intensity units (FIU). All measurements were carried out in a Fluostar Optima spectrofluorometer (BMG Technologies, Offenburg, Germany) or using a LS-50B luminescence spectrometer (Perkin-Elmer Life Sciences) and analyzed using an FL Winlab software package.

SDS-PAGE and Western Blot Analysis—Cell lysate proteins were separated by electrophoresis on 12% polyacrylamide gels and subjected to Western blot analysis for FasL detection as described previously (36). For cytochrome *c* and caspase-8 detection, 10% polyacrylamide gel was used, but for iNOS, 7.5% polyacrylamide gel was required. All primary antibodies were diluted to 1:1,500 except anti-FasL, which was diluted to 1:2,000; for secondary antibody goat anti-rabbit IgG conjugated with horseradish peroxidase at 1:5,000 dilution was used. Reactive bands were visualized by using a Vector Immuno Peroxidase substrate kit.

Statistical Analysis—Paired comparisons of the data were conducted using a paired *t* test, and all data are presented at mean values ± S.E. Differences were considered significant at a 0.05 level of confidence.

RESULTS

Spermatogenic Cell Death Occurs after 17β-Estradiol Exposure in Vitro—Fig. 1*A*, *a* and *b*, shows flow cytometric analyses of the cell preparation used for this study. The percentages of haploid and diploid cells were 80 and 20%, respectively (Fig. 1*Aa*). Fig. 1*Ab* is a representation of the cell population on a dot plot to identify the various cell types. Among the diploid cells represented as *black dots*, there are two distinct populations, a population with 4C DNA content representing spermatocytes and a population with 2C DNA content comprising of secondary spermatocytes and spermatogonia. Secondary spermatocyte numbers being very low in the testis, the 2C population primarily represents the spermatogonia. Postmeiotic haploid cells with the 1C DNA amount represented as *gray dots* were identifiable separately from the other two groups and consisted of the largest population representing spermatids (Fig. 1*Ab*). Under the microscope, the size, shape, and chromatin pattern of nuclei, the presence of metaphase figures, and the presence of the acrosomal cap were used to identify the cell types. Fig. 1*Ac* shows the Nomarski photomicrograph of the cell population used for the studies, and Fig. 1*Ad* is the Nomarski recording overlapped with Hoechst staining, which clearly shows the nuclear material making identification easier. Pachytene spermatocytes were the largest cells with a typical dispersed chromatin; round spermatids were clearly distinguishable by their acrosomal caps and spermatogonia by size and spherical nuclei (37).

Two doses of estradiol, 10^{-8} and 10^{-7} M, were used to check the ability of the cells to survive in the presence of the hormone. There was about an 80% reduction in cell survival at 10 h after initiation of estradiol treatment with both doses; therefore, in the absence of any significant difference between the doses in terms of cell death, we decided to use 10^{-8} M 17β-estradiol for all further studies. Fig. 1*Ba* represents cell death percentages obtained over a 10-h time period with 10^{-8} M 17β-estradiol. There was a progressive decrease in cell viability which reached about 20% of survival at 10 h postestradiol treatment (Fig. 1*Ba*). Arguably, if estrogen was exerting its action through its receptors and not through any other indirect mechanisms, the presence of estrogen receptor modulators during exposure to estrogen should ideally inhibit estrogen action. We

are, *(i)*, PI-positive cells; *(ii)*, PI- and annexin-positive cells (late apoptotic); *(iii)*, unstained cells; *(iv)*, annexin-positive cells (early apoptotic). Experimental groups are indicated in the figure. Note that in the presence of 10 nM tamoxifen (*Tam*) 17β-estradiol was unable to induce phosphatidylserine exposure in a significant number of cells (*c*). *B*, microphotographs showing annexin-labeled cells. *a*, *d*, and *g*, Nomarski photomicrographs; *b*, *e*, and *h*, annexin conjugated to Alexa Fluor labeling of cells; *c*, *f*, and *i*, PI stain. *a–c* show control cells with no PI or annexin stain; *d–f* show estradiol-treated cells with annexin-positive foci on the cell surface as evident from dot fluorescence (indicated by *arrows*) on the cells; *g–i*, estradiol and tamoxifen treatment showing no annexin labeling. *C* and *D*, DNA fragmentation and laddering. After 8 h of 17β-estradiol exposure, cells positive for DNA fragmentation increase as evident by the significant shift (*a*). Note that the number of TUNEL-positive cells is reduced when 10 nM tamoxifen was present during 17β-estradiol exposure. The *percentages* within *parentheses* represent the number of viable cells. Data are representative of three experiments. *c*, genomic DNA prepared from control and treated cells were run on a 1% agarose gel. DNA ladders were visible after 9 and 10 h of exposure to 17β-estradiol compared with control samples where a clear genomic DNA band is visible. *M* represents molecular weight markers. *D*, *a* and *b*, control at 8 h; *c* and *d*, estradiol treatment at 8 h. Note staining of spermatocytes (*SC*) and spermatogonia (*SG*); *e* and *f*, estradiol treatment in the presence of tamoxifen at 8 h. Note the reduction of TUNEL-positive cells; *g* and *h*, control at 10 h; *i* and *j*, estradiol treatment at 10 h. Note staining of spermatocytes and spermatids (*ST*); *k* and *l*, estradiol treatment in the presence of tamoxifen at 10 h. Note the lack of TUNEL-positive cells. Microphotographs are representative of three experiments.

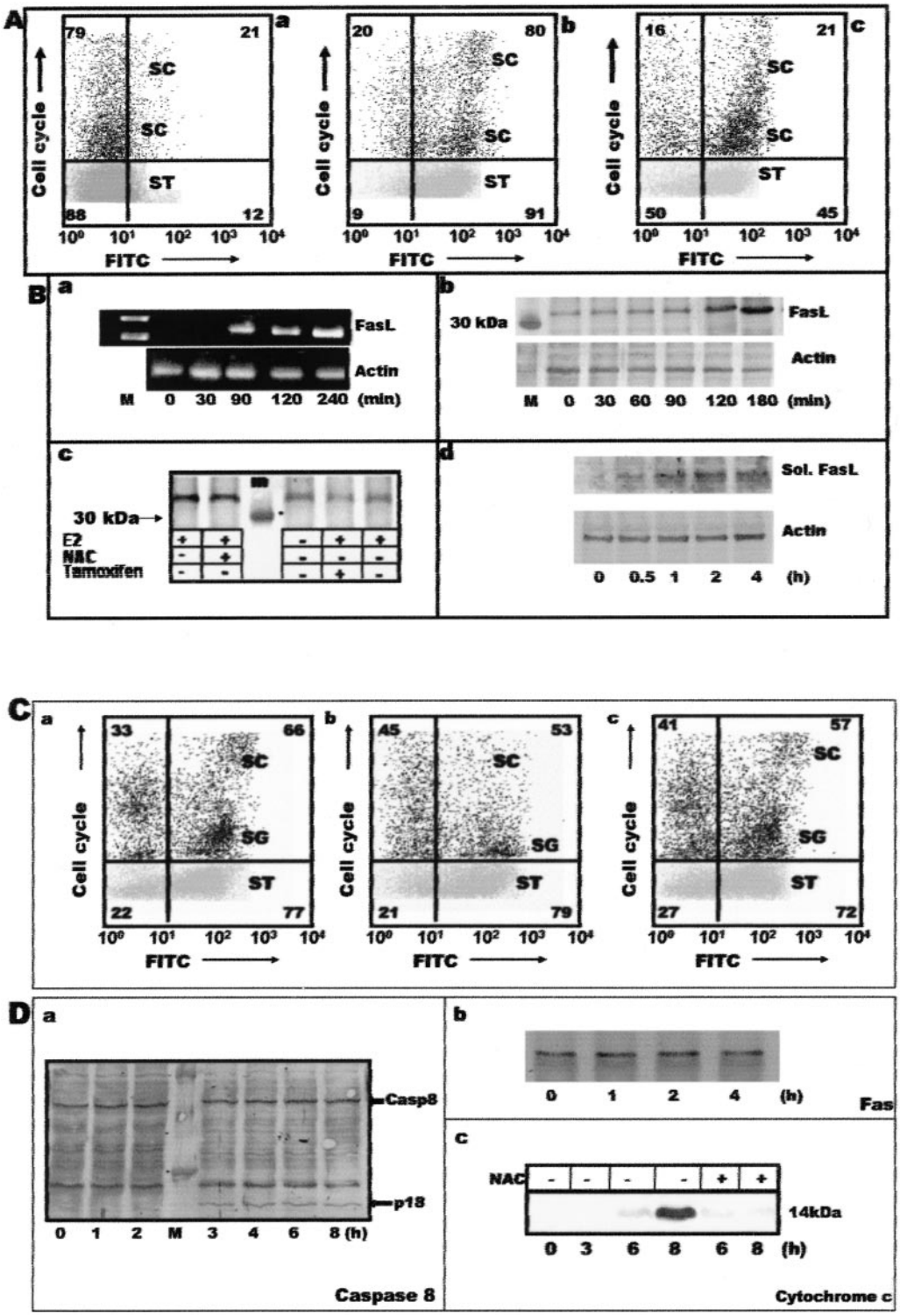

FIG. 3. **FasL is up-regulated in response to 17β-estradiol.** *A*, staining of spermatogenic cells with anti-FasL antibody. *a*, control cells staining for FasL at 2 h; *b*, spermatogenic cells staining after estradiol treatment at 2 h. Note the significant shift in both the diploid and the haploid populations representing increased staining for FasL. *c*, reduction in the number of cells staining for FasL when estradiol was given with 10 nM tamoxifen. The *numbers* in each *quadrant* represent the percentages of cells. The *upper two quadrants* represent total diploid cells, and the *lower two quadrants* represent total haploid cells. *B*, changes in FasL expression. *a*, reverse transcription-PCR of FasL and actin mRNA from spermatogenic cells at different time points after 17β-estradiol exposure. Note the increase in FasL mRNA from 90 min onward. *b*, Western blots of spermatogenic cell cytosol at different time points probed with anti-FasL antibody after exposure to 17β-estradiol. Note the gradual increase in reactivity with time. The *lower blot* shows actin reactivity of the same extracts. *c*, reactivity of anti-FasL antibody to extracts from cells treated as indicated in the figure. Note that NAC was unable to reduce FasL expression. *d*, spermatogenic cell culture media analyzed for soluble FasL. Data are representative of a minimum of three experiments. *C*, expression of Fas and cleavage of caspase-8. *a*, dot plots demonstrating staining of spermatogenic cells with anti-Fas antibody. Data are representative of four experiments. *a*, control; *b*, 17β-estradiol treatment; *c*, 17β-estradiol given with tamoxifen. Note no change in staining in the presence of estradiol in any population of cells. *D*, *a*, Western blots of spermatogenic cell extracts showing caspase-8 cleavage (*Casp8*; p18) from 3 h onward after 17β-estradiol treatment. *M*, molecular weight markers. *b*, Western blots of **s**permatogenic cell extracts probed with anti-Fas antibody showing no changes in Fas expression with time. *c*, reactivity of anti-cytochrome *c* antibody to spermatogenic cell extracts. Note the strongest reactivity at 8 h and the ability of NAC to reduce anti-cytochrome *c* reactivity. All experiments are representative of a minimum of three repeats.

tried five different doses of tamoxifen (5, 10, 20, 50, an 100 nM), an estrogen receptor modulator, during estradiol exposure and found that 10 nM was the lowest possible dose that could be used. The presence of tamoxifen reduced cell death significantly, 70% of the cells being viable at 10 h in the presence of tamoxifen (Fig. 1*Ba*). Fig. 1*B*, *b–d*, shows microphotographs of cells stained with PI in different treatment groups. At 10 h the types of cell dying were spermatids, spermatogonia, and spermatocytes (Fig. 1*Bc*), which was not visible in controls (Fig. 1*Bb*). When given along with estradiol, tamoxifen could reduce cell death (Fig. 1*Bd*). Fig. 1*C*, *a–c*, shows flow cytometric analysis of spermatogenic cell death at 10 h. All three spermatogenic cell populations were affected by estradiol over the period of 10 h (Fig. 1*Cb*), visible by a shift toward increased PI staining compared with controls (Fig. 1*Ca*). It is to be noted that although 87% of the haploid cells were PI-positive at 10 h, the percentage of diploid cells staining for PI was 64% (Fig. 1*Cb*) after estradiol treatment. Tamoxifen could inhibit the ability of estradiol to induce cell death significantly in both populations, the effective reductions being 34% in diploid and 53% in the haploid cells (Fig. 1*Cc*). Notably, both the spermatogonial and spermatocyte cell population suffered cell death and could be rescued by tamoxifen.

This part of the study therefore demonstrated (i) the ability of 17β-estradiol to induce spermatogenic cell death in both the haploid (round spermatid) and the diploid (spermatocytes and spermatogonia) cells in the absence of testicular somatic cells and (ii) that the effect of estradiol was receptor-mediated as evidenced by the ability of the estrogen receptor modulator tamoxifen to prevent 17β-estradiol-induced death.

17β-Estradiol-induced Cell Death Occurs through Apoptosis—Having demonstrated the ability of 17β-estradiol to affect cell survival *in vitro*, it was important to determine whether the death was necrotic or apoptotic. First we investigated the expression of apoptotic phenotypes by examining markers such as exposure of phosphatidylserine, DNA fragmentation, and DNA laddering (38) in the total population comprising both haploid and diploid cells. Treatment with 17β-estradiol resulted in phosphatidylserine exposure (annexin-V-positive) in about 75% of cells (including both early and late apoptotic cells) by 8 h (Fig. 2*Ab*) compared with controls (Fig. 2*Aa*) where only 12% of the population showed annexin-positive plasma membrane. The presence of tamoxifen during the 17β-estradiol treatment reduced the number of annexin-positive cells (Fig. 2*Ac*) compared with that observed with 17β-estradiol only (Fig. 2*Ab*). Microscopic analysis revealed that although the untreated group did not show any annexin-positive cells (Fig. 2*B*, *a–c*), the treated group showed both spermatocytes and spermatids staining for annexin-V (Fig. 2*B*, *d–f*). There was no significant staining with annexin-V in the groups that were exposed to tamoxifen at the same time as estradiol (Fig. 2*B*, *g–i*). TUNEL assay showed a significant number of spermatogenic cell nuclei with fragmented DNA at 9 h in 17β-estradiol-exposed groups (Fig. 2*Ca*) compared with groups where tamoxifen was used (Fig. 2*Cb*). Genomic DNA prepared from spermatogenic cells after 9 and 10 h of 17β-estradiol treatment showed distinct DNA laddering compared with 0 h controls (Fig. 2*Cc*). Fig. 2*D* shows spermatogenic cells stained for TUNEL. The most predominant group staining for TUNEL at 6 h were the pachytene spermatocytes (Fig. 2*D*, *c* and *d*). None of these cells was stained in controls except a few spermatogonia (0.2%) (Fig. 2*D*, *a* and *b*). At the 8 h time point, in addition to spermatocytes, spermatids stained in significant numbers (Fig. 2*D*, *i* and *j*) compared with controls (Fig. 2*D*, *g* and *h*). The number of TUNEL-positive cells was reduced in groups where tamoxifen was present during estradiol exposure (Fig. 2*D*, *e* and *f*, and *k* and *l*). Thus, from the above data, it was evident that estradiol could induce an apoptotic phenotype in both the haploid and the diploid spermatogenic cells which included (i) phosphatidylserine exposure, (ii) DNA fragmentation, and (iii) laddering of the genomic DNA.

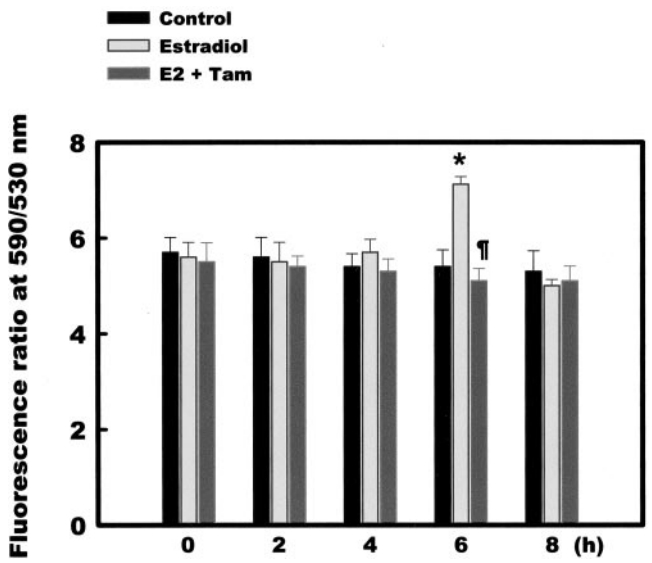

FIG. 4. **17β-Estradiol induces a transient mitochondrial hyperpolarization.** After various treatments as indicated in the figure, spermatogenic cells were loaded with the potentiometric probe JC-1, and $\Delta\psi_m$ was measured. A transient increase in mitochondrial polarization was observed at 6 h after 17β-estradiol exposure; however, when tamoxifen was given concurrently during 17β-estradiol exposure (*E2+Tam*) this hyperpolarization did not occur. *, E2 at 6 h *versus* control; ¶, E2 + Tam at 6 h *versus* E2 at 6 h, $p < 0.05$. $n = 3$; data are the mean ± S.E.

FasL Up-regulation Occurs Followed by Caspase-8 Cleavage after Estradiol Exposure—Because our *in vivo* studies demonstrated an up-regulation of FasL in response to 17β-estradiol, we first checked whether a similar increase could be observed *in vitro* or a different pathway was stimulated. When cells were stained with anti-FasL antibody 3 h after estradiol treatment and scanned using flow cytometry, it was apparent that bulk of all three populations stained for FasL as evident by a significant increase in the number of stained cells from 21 to 80% of the diploid and 12 to 91% of the haploid cells (Fig. 3*Ab*). The presence of 10 nM tamoxifen reduced this staining percentage significantly (Fig. 3*Ac*), thus providing evidence that FasL up-regulation was induced through an estrogen receptor-mediated mechanism. About 21% of diploid and 12% of haploid cells showed constitutive expression of FasL (Fig. 3*Aa*). In support of the above observation we found that an increase in the expression of FasL mRNA occurred within 90 min of exposure to estradiol (Fig. 3*Ba*). The increase in actual FasL protein became apparent at 120 min postestradiol exposure (Fig. 3*Bb*) at which point a difference from the constitutively expressed levels was evident (Fig. 3*Bb*). Consequently, confirmation of estrogen receptor dependence was checked, and in the presence of tamoxifen a decrease in the FasL protein was detectable on the Western blot (Fig. 3*Bc*). The presence of NAC, an antioxidant, did not interfere with FasL expression. FasL is sometimes cleaved by metalloproteases to release soluble FasL (39), which is an important phenomenon in the testis. Soluble FasL was detectable in the culture medium, and an increased release with time was recorded (Fig. 3*Bd*).

Consequent to investigations with FasL, we tried to establish whether there was a change in Fas protein. Flow cytometric analysis of the cell populations showed that Fas expression did not change significantly either in the haploid or the diploid

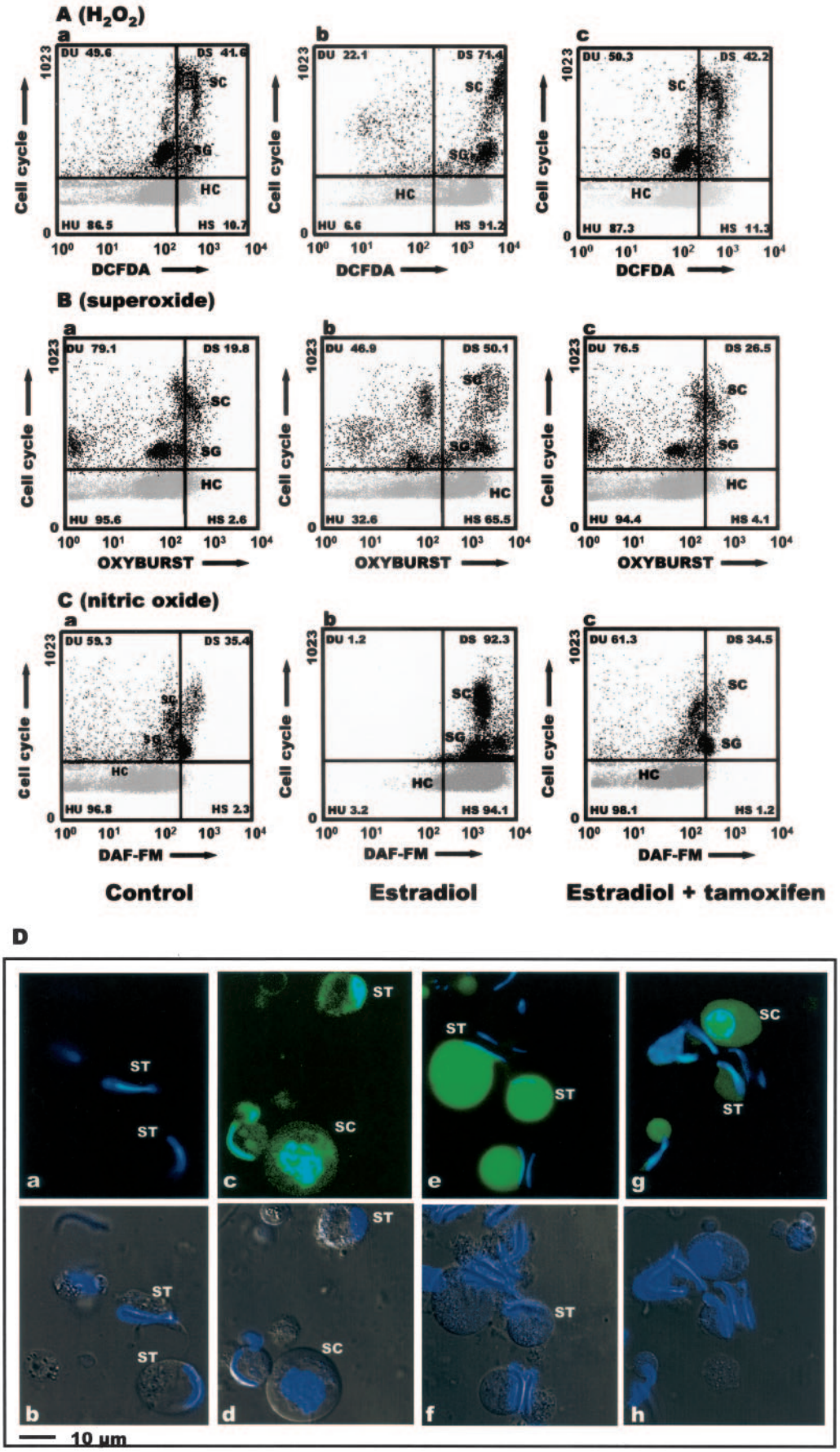

FIG. 5. **ROS and nitrogen species increase after estradiol exposure.** *A*, generation of H_2O_2. Dot plots show the spermatogenic cell populations generating H_2O_2; *a*, untreated; *b*, treated with estradiol; *c*, treated with estradiol and tamoxifen. The *numbers* in each *quadrant* represent the percentages of cells. The *upper two quadrants* represent total diploid cells, and the *lower two quadrants* represent total haploid cells.

population in response to estradiol treatment (Fig. 3*Cb*) compared with control expression (Fig. 3*Ca*). Western blot analysis of cell extracts from 0 to 4 h of estradiol exposure also showed no change in Fas protein profile (Fig. 3*Db*). The ligation of FasL with Fas recruits death domain proteins that lead to the activation of caspase-8 (38). Caspase-8 cleavage to an 18-kDa fragment was evident from 3 h onward (Fig. 3*Da*). Caspase-8 cleavage can activate caspase-3 directly or go through the mitochondrial pathway to activate caspase-3 via the release of cytochrome *c* into the cell cytosol (38). An increase in cytochrome *c* immunoreactivity in treated spermatogenic cell cytosol was strongly visible at 8 h after 17β-estradiol exposure with a faint reaction visible at 6 h (Fig. 3*Dc*). The presence of NAC reduced the reactivity of the cytosol toward anti-cytochrome *c*, showing that NAC was able to interfere with the release of cytochrome *c* (Fig. 3*Dc*).

The above experiments clearly demonstrated that (i) FasL expression increased in both the haploid and the diploid cells in response to estradiol; (ii) Fas expression remained unaltered; (iii) caspase-8 cleavage occurred consequent to estradiol exposure; and (iv) cytochrome *c* release was observed, suggesting involvement of the mitochondria.

Mitochondrial Hyperpolarization Is Induced by 17β-Estradiol—The release of cytochrome *c* indicated mitochondrial involvement; therefore, we attempted to study the mitochondrial changes in terms of alterations in mitochondrial polarization, which would be indicative of the status of mitochondrial function. Simultaneous measurement of J-aggregate (indicative of intact mitochondria) and J-monomer (indicative of de-energized mitochondria) formation expressed as the ratio of 590:530 fluorescence showed an increase of $\Delta\psi_m$ at 6 h in the groups exposed to 17β-estradiol compared with the $\Delta\psi_m$ of controls (Fig. 4). Interestingly, this hyperpolarization was transient in nature and was not measurable at 8 h, at which point the potential returned to normal levels comparable with controls. The $\Delta\psi_m$ increase could be inhibited by the presence of tamoxifen, indicating that an estrogen-receptor interaction was required for mitochondrial hyperpolarization (Fig. 4).

Up-regulation of NO, Superoxide, and H_2O_2 Occurs after Exposure to 17β-Estradiol—Mitochondrial changes are often associated with ROS generation, therefore we estimated the extent of superoxide and H_2O_2 generated in response to 17β-estradiol. In addition, we also checked changes in NO levels because estrogen increases NO under certain circumstances (40). It was evident that H_2O_2 increased in all three cell populations as shown by the increase in the number of cells staining for H_2DCFDA (Fig. 5*Ab*) compared with controls (Fig. 5*Aa*). Interestingly, about 42% of the diploid cells exhibited constitutive H_2O_2 generation, which increased to a higher level after estradiol exposure, as was evident from the significant shift in staining intensity (Fig. 5*Ab*). When tamoxifen was present, the shift in staining reverted to control levels (Fig. 5*Ac*). Superoxide production increased in both the haploid and the diploid cells, the increase being 2–65% in haploid cells and 19–50% in diploid cells (Fig. 5*Bb*) compared with no treatment (Fig. 5*Ba*). Interestingly, although this change was significant, 46% of diploid cells did not generate superoxide, and this included both spermatocytes and spermatogonia. The presence of tamoxifen was able to reduce the percentage of cells generating superoxide (Fig. 5*Bc*), affecting both the diploid and the haploid population. The most dramatic increase involving all cell types was observed in the generation of NO, where the percentage of cells stained in estradiol-treated groups increased from 35 to 92 in diploid population and from 3 to 94 in the haploid population (Fig. 5*Cb*) compared with controls (Fig. 5*Ca*). Tamoxifen could prevent NO generation in both the haploid and the diploid cells (Fig. 5*Cc*). Fig. 5*D* shows fluorescence micrographs demonstrating the generation of superoxide (Fig. 5*D*, *c* and *d*), NO (Fig. 5*D*, *e* and *f*), and H_2O_2 (Fig. 5*D*, *g* and *h*) in spermatogenic cells. Therefore, the above data demonstrated that (i) NO, H_2O_2, and superoxide were generated in response to 17β-estradiol by all three population of cells, but about 46% of diploid cells were not involved in the generation of superoxide, whereas the bulk of the haploid cells stained for both; (ii) NO was generated by more that 90% of the haploid and the diploid cells in response to estradiol; and (iii) tamoxifen reduced the increase in generation of superoxide, NO, and H_2O_2.

Inhibition of Superoxide and NO Results in the Inhibition of Mitochondrial Hyperpolarization—We next attempted to delineate whether changes in H_2O_2 or superoxide or NO or a combination was responsible for the mitochondrial hyperpolarization and eventual cell death. For this, antioxidant NAC was used to see whether it could reduce the levels of the above molecules, and if reduction was present whether this was related to hyperpolarization. We found that a 2-h preincubation with NAC could effectively reduce H_2O_2 levels (Fig. 6*A*), but a 1-h preincubation was ineffective in doing so; in contrast, both preincubation times effectively reduced superoxide and NO generation (Fig. 6, *B* and *C*). When $\Delta\psi_m$ was checked after estradiol treatment, it was found that preincubation with NAC for either 1 or 2 h was able to reduce $\Delta\psi_m$ increase (Fig. 6*D*). Therefore, if H_2O_2 was responsible for hyperpolarization, then a 1-h preincubation with NAC, which is unable to reduce H_2O_2, would have been ineffective in reducing $\Delta\psi_m$. This pointed toward the involvement of superoxide or NO or a combination of both being responsible for the hyperpolarization.

A selective inhibitor for iNOS was subsequently used to reduce NO generation, and the effects on $\Delta\psi_m$ were assessed. In addition, NO- and superoxide-generating systems were used to expose the cells to either or both of the molecules to determine whether NO or superoxide acting by themselves or in combination could influence $\Delta\psi_m$. A 120-min preincubation with AG (E2+AG), the iNOS inhibitor, prevented hyperpolarization observed at 6 h; however, cells in this group showed hyperpolarized mitochondria at 8 h (Fig. 6*E*), indicating that addition of AG delayed the onset of hyperpolarization. This correlated with the level of NO generated (Fig. 6*F*) because AG inhibited the NO increase that occurred from 4 h onward. The addition of AG for a second time at 4 h (E2+AG+AG) after the earlier addition was able to inhibit further the NO levels and stopped the increase in $\Delta\psi_m$, revealing that a sustained lowering of NO levels was able to inhibit hyperpolarization (Fig. 6, *F* and *E*).

Note the significant shift to increased fluorescence in all generations of the spermatogenic cells. *B*, status of superoxide. Cells positive for superoxide are shown in dot plots; *a*, untreated; *b*, treated with estradiol; *c*, treated with estradiol and tamoxifen. Note the significant shift to increased fluorescence in a substantial percentage of cells in all generations of the spermatogenic cells. *C*, production of NO. Dot plots show the spermatogenic cell populations positive for NO; *a*, untreated; *b*, treated with estradiol; *c*, treated with estradiol and tamoxifen. Data are representative of a minimum of three experiments. *SC*, spermatocytes; *SG*, spermatogonia; *ST*, spermatids. *HU*, haploid unstained; *DU*, diploid unstained; *HS*, haploid stained; *DS*, diploid stained. *D*, photomicrographs of cells showing the generation of superoxide, NO, and H_2O_2. The Nomarski photographs are overlaps of the *blue* and transmission channel showing Hoechst staining combined with Nomarski. *a* and *b*, fluorescence and Nomarski photomicrographs, respectively, of untreated cells; *c* and *d*, fluorescence and Nomarski photomicrographs of cells treated with 17β-estradiol stained for superoxide production with OxyBURST Green; *e* and *f*, fluorescence and Nomarski photomicrographs of cells treated with 17β-estradiol stained for NO with DAF-FM; *g* and *h*, fluorescence and Nomarski photomicrographs of cells treated with 17β-estradiol stained for H_2O_2 with CM-H_2DCFDA.

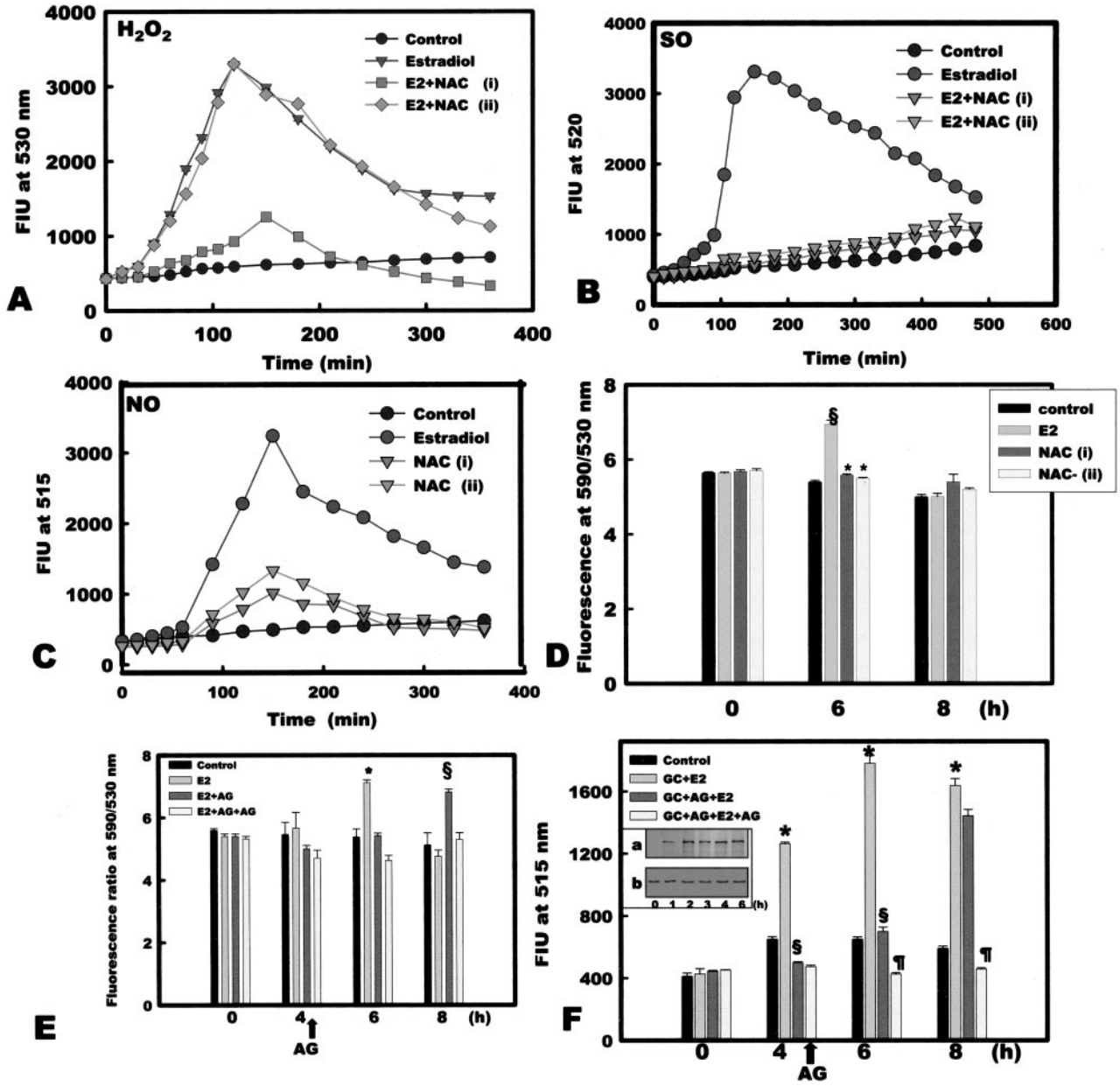

FIG. 6. **Effects of NAC and AG show superoxide and NO production.** *A*, H_2O_2 generation in the presence of NAC. H_2O_2 generation after addition of 17β-estradiol shows peak H_2O_2 produced at 120 min. The presence of NAC was able to lower H_2O_2 production when added 2 h prior to exposure of the cells to estradiol but not with only a 1-h preincubation. $n = 3$, data are the mean ± S.E. *B*, superoxide generation in the presence of NAC. Superoxide production after the addition of 17β-estradiol shows that peak superoxide is produced at 150 min. The presence of NAC was able to lower superoxide production when added 1 or 2 h prior to exposure of the cells to 17β-estradiol. $n = 3$, data are mean ± S.E. *C*, NO production in the presence of NAC. NO generation in spermatogenic cells measured with DAF-FM after the addition of 17β-estradiol shows that peak NO is generated at 150 min. The presence of NAC was able to lower NO production when added 1 or 2 h prior to exposure of the cells to estradiol. $n = 3$, data are mean ± S.E. *D*, $\Delta\psi_m$ after estradiol and NAC treatment. the *bar graph* shows the effect of NAC on mitochondrial hyperpolarization. The hyperpolarization induced by 17β-estradiol could be reduced to control levels when NAC preincubation was given for 1 *(i)* or 2 h *(ii)*. $n = 3$, data are mean ± S.E. §, E2 at 6 h *versus* control, $p < 0.05$; *, NAC at 6 h *versus* E2 (1 and 2 h preincubation). *E*, $\Delta\psi_m$ after estradiol and AG treatment. Preincubation with AG for 120 min prior to 17β-estradiol addition (*E2+AG*) delayed the onset of hyperpolarization by 2 h. A second addition of AG at 4 h (*E2+AG+AG*) to the group already exposed to AG, as indicated by the *arrow*, could delay the hyperpolarization as observed until 8 h, $n = 3$, data are mean ± S.E. *, E2+AG (120 min preincubation) and E2+AG+AG (second addition at 4 h) *versus* E2 at 6 h, $p < 0.05$; §, E2+AG (120-min preincubation) *versus* E2 at 8 h, $p < 0.05$. *F*, NO production after estradiol treatment in the presence of AG. Corresponding measurement of NO production by the spermatogenic cells in the above experiment (shown in *E*) shows that the presence of AG was able to block NO production effectively, $n = 3$, data are mean ± S.E. *, E2 at 4, 6, and 8 h *versus* control at 4, 6, and 8 h, $p < 0.05$; §, E2 + AG at 4 and 6 h *versus* E2 at 4 and 6 h, $p < 0.05$; ¶, E2+AG+AG at 6 and 8 h *versus* E2, $p < 0.05$. *Inset*. *a*, Western blots of spermatogenic cell cytosol using anti-iNOS antibody show an increase in iNOS levels from 1 h onward. The figure is representative of three repeats. *b*, actin staining of the same lanes of the blots.

The increase in NO provided a possibility that iNOS levels may have increased because estrogens are known to increase iNOS levels through an increase in expression. In support of this, an increased reactivity of anti-iNOS antibody toward the spermatogenic cell cytosol was observed after 1 h of exposure (Fig. 6*F*, *inset a*). Therefore, the ability of AG to delay hyperpolarization raised two possibilities: either NO by itself was enough to cause mitochondrial hyperpolarization or NO was interacting with superoxide to form peroxynitrite, which was responsible for hyperpolarization. This part of the data shows that (i) a 60-min

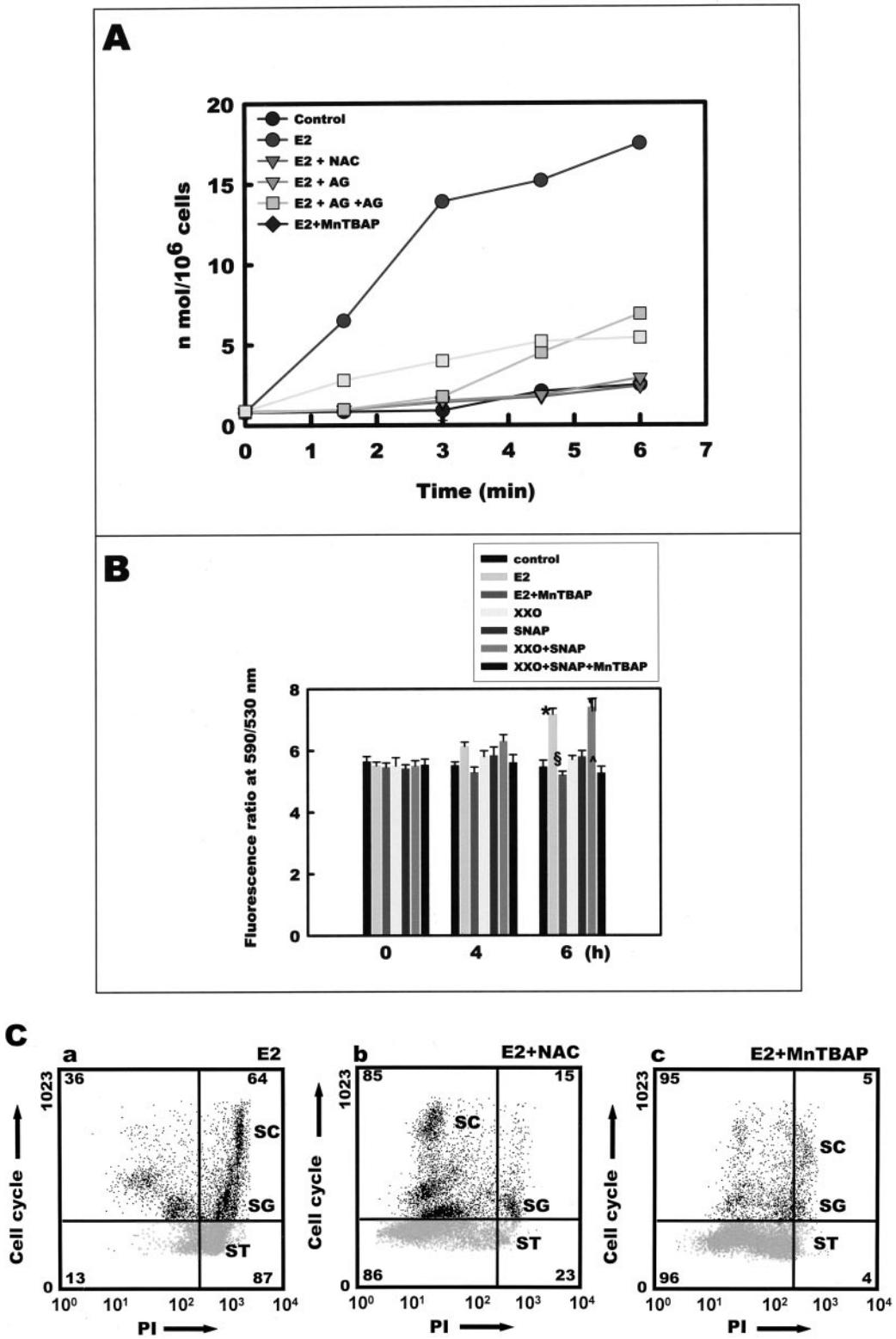

FIG. 7. **Estrogen increases nitrite levels, and NO and superoxide generated together cause a transient mitochondrial hyperpolarization.** *A*, nitrite levels. The figure shows nitrite levels after various treatments. Note that 17β-estradiol treatment results in an increased nitrite level; however, the presence of AG, MnTBAP, and NAC is able to reduce these levels, $n = 3$, data are mean ± S.E. E2 + AG (120-min preincubation); E2+AG+AG (second addition at 4 h). *B*, status of $\Delta\psi_m$. The figure shows the status of $\Delta\psi_m$ when MnTBAP was used during estrogen exposure. The figure also shows the effect of NO generation with SNAP and superoxide with xanthine/xanthine oxidase (XXO) on $\Delta\psi_m$ when generated separately or in combination (*XXO + SNAP*) in spermatogenic cell cultures. It is evident that spermatogenic cell mitochondria undergo hyperpolarization when there is a combined generation of superoxide and NO (*XXO + SNAP*). MnTBAP, the peroxinitrite scavenger, was able to inhibit hyperpolarization when given with XXO and SNAP (*XXO+SNAP+MnTBAP*), $n = 3$, data are mean ± S.E. *, E2 *versus* control; §, E2+ MnTBAP *versus* E2; ¶, XXO + SNAP *versus* control, $p < 0.05$; [caret], XXO+SNAP+MnTBAP *versus* XXO+SNAP, $p < 0.05$. E2, 17β-estradiol. *C*, cell viability after estrogen treatment in the presence of NAC and MnTBAP. Shown is the effect of estradiol (*a*), estradiol in the presence of NAC (*b*), and estradiol in the presence of MnTBAP (*c*) on cell viability. Note the significant reduction in cell death with NAC and MnTBAP from 64 to 15 and 5%, respectively. *Numbers* in the *quadrants* represent percentages of cells in the *upper* and *lower quadrants*. Data are representative of three repeats.

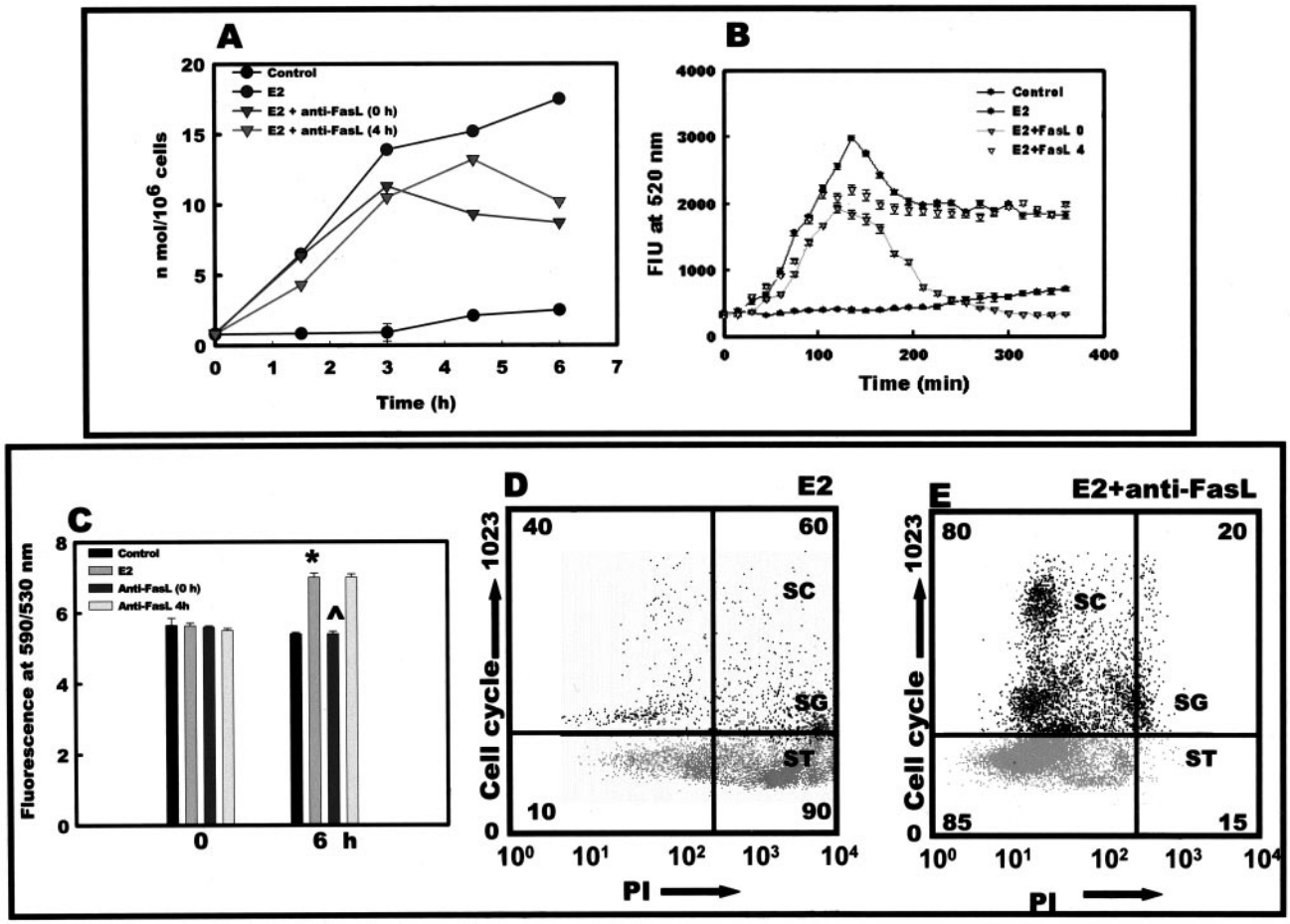

FIG. 8. **Effect of anti-FasL antibody on nitrites, superoxide, $\Delta\psi_m$, and cell viability.** *A*, anti-FasL antibody induced reduction of nitrites when added along with estradiol. *B*, superoxide generation in the presence of anti-FasL shows that there is no substantial reduction of superoxide generation in the presence of anti-FasL when added at the time of estradiol addition for the first 3 h. Addition after 4 h showed no effect in superoxide reduction. Data are mean ± S.E. of four observations. *C*, anti-FasL is able to reduce $\Delta\psi_m$ when added at 0 h with estradiol but not when added at 4 h after estradiol addition. *, E2 *versus* control (0 h); anti-FasL 0 h *versus* E2, $p < 0.05$. *D*, cell death increase cause by exposure to estradiol. *E*, cell death increase caused by exposure to estradiol is reduced if anti-FasL is present during estradiol exposure (added at the time of estrogen exposure). The *numbers* in each *quadrant* represent the percentages of cells. The *upper two quadrants* represent total diploid cells, and the *lower two quadrants* represent total haploid cells.

preincubation with NAC was sufficient to reduce NO and superoxide but not H_2O_2; (ii) mitochondrial hyperpolarization was prevented when preincubation with NAC for 60 or 120 min was carried out; (iii) AG was successful in reducing hyperpolarization, and iNOS expression increased in response to estradiol.

Nitrite Levels Increased in Response to Estradiol, and Scavenging of Nitrites Reduced Mitochondrial Hyperpolarization—An actual increase in nitrite levels was detected with 17β-estradiol exposure which was reduced in the presence of MnTBAP, NAC, and AG (Fig. 7*A*). When MnTBAP was given along with 17β-estradiol, it resulted in an inhibition of hyperpolarization (Fig. 7*B*). These results were an indication that nitrites were related to mitochondrial destabilization. A possible way to dissect the role of NO and superoxide was to use NO- or superoxide-generating systems to see the response of spermatogenic cell mitochondria. This system was used because NO and superoxide can combine to form peroxynitrite. Xanthine/xanthine oxidase was used to generate superoxide, and SNAP was used to generate NO in spermatogenic cell cultures. Prior to initiating these experiments, the amount of NO and superoxide generated by NO- and superoxide-generating systems was determined and compared with the levels generated by 17β-estradiol in spermatogenic cells. Xanthine/xanthine oxidase required to generate an amount of superoxide equivalent to that induced by 17β-estradiol was 50 μM xanthine and 0.05 μM xanthine oxidase and that of SNAP was 4 μM. Although individually either of the compounds was unable to induce significant hyperpolarization, together they were able to increase $\Delta\psi_m$ (Fig. 7*B*), which was effectively prevented in the presence of MnTBAP. When added to the spermatogenic cell culture, H_2O_2 did not cause any hyperpolarization (control, 6 ± 0.3; H_2O_2, 6.2 ± 0.43, $n = 3$). When NAC and MnTBAP were used with estradiol and cell viability was checked, a significant reduction in cell death was observed (Fig. 7*C*, *b* and *c*) compared with that observed with estradiol (Fig. 7*Ca*).

Therefore, the above data show that (i) nitrites were generated in response to estradiol; (ii) simultaneous generation of NO and superoxide resulted in hyperpolarization that was prevented by MnTBAP; and (iii) MnTBAP and NAC were able to prevent cell death.

Anti-FasL Antibody Inhibits Mitochondrial Hyperpolarization, Nitrite Generation, and Cell Death—Anti-FasL antibody was used to delineate the events that involved Fas-FasL ligation. If estradiol was added in the presence of anti-FasL antibody, there was a reduction in nitrite generation (Fig. 8*A*). However, when superoxide was measured in a similar situation, until about 3 h superoxide generation could not be prevented by the antibody. Addition of the antibody 4 h after addition of estradiol did not prevent superoxide production (Fig. 8*B*). Mito-

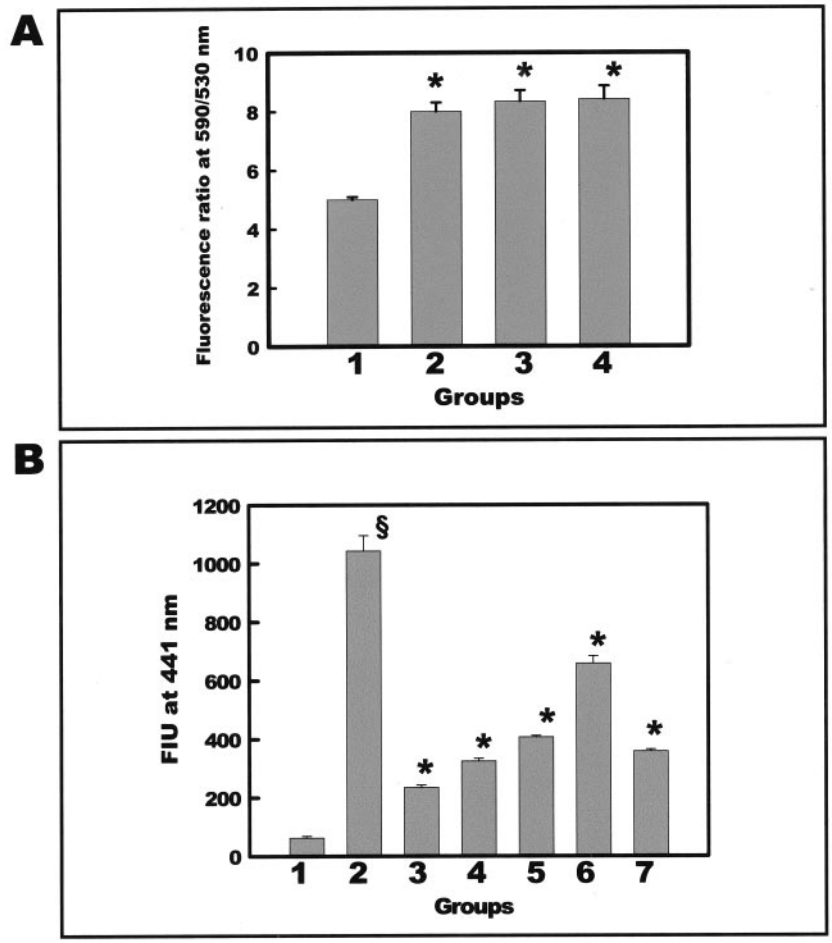

FIG. 9. **Caspase-8 inhibition shows no effect on $\Delta\psi_m$, and NAC and AG treatment leads to abrogation of caspase-3 activity.** *A*, effects of caspase-8 inhibitor on $\Delta\psi_m$. The figure shows the inability of caspase-8 inhibitor Z-LETD-FMK to reduce mitochondrial hyperpolarization. *1*, control; *2*, 17β-estradiol; *3*, Z-LETD-FMK (20 μM) + 17β-estradiol; *4*, Z-LETD-FMK (40 μM) + 17β-estradiol, $n = 3$, data are mean ± S.E. * $p < 0.05$. *B*, effects on caspase-3 activity. Inhibition of caspase-3 activity by different treatments. *1*, control; *2*, 17β-estradiol; *3*, NAC + 17β-estradiol; *4*, AG + 17β-estradiol at 0 h; *5*, 17β-estradiol + AG added at both 0 and 4 h; *6*, caspase-8 inhibitor Z-LETD-FMK + 17β-estradiol; *7*, tamoxifen + 17β-estradiol, $n = 3$, data are mean ± S.E. §, 17β-estradiol *versus* control; *, NAC, tamoxifen, AG at 0 h, AG at 0 and 4 h, caspase-8 inhibitor Z-LETD-FMK *versus* E2, $p < 0.05$.

chondrial hyperpolarization was inhibited by the anti-FasL antibody when added concomitantly with estradiol (Fig. 8*C*). This antibody was also able to reduce cell death (Fig. 8*E*) compared with estradiol-induced death (Fig. 8*D*), thus establishing a relationship between Fas receptor ligation and cell death.

Inhibition of Caspase-8 Reduces Cell Death but Not Mitochondrial Hyperpolarization—When we used the caspase-8 inhibitor Z-LETD-FMK, there was no inhibition of mitochondrial hyperpolarization (Fig. 9*A*). Caspase-3 cleavage and activation are downstream from caspase-8 activation, and therefore inhibition of caspase-8 should prevent the cleavage of caspase-3. A significant increase in caspase-3 activity in the estrogen-treated groups was noted which could be prevented by NAC, AG, tamoxifen, and the caspase-8 inhibitor (Fig. 9*B*). Therefore, this showed that (i) caspase-8 activation had no effect on mitochondrial hyperpolarization and (ii) caspase-3 activity could be prevented by inhibition of either caspase-8 or NO and superoxide generation.

In the Absence of Fas, 17β-Estradiol Is Not Able to Induce Mitochondrial Hyperpolarization, ROS Generation, and Cell Death—Although we used the rat as a model organism for the source of spermatogenic cells, we used B6.MRL.lpr (B6-lpr,lpr) mice that are deficient in Fas receptor to establish the absolute requirement of Fas in 17β-estradiol-induced hyperpolarization in spermatogenic cells. For controls we used wild type C57BL/6 (B6) mice. Clearly, in the controls, at 6 h, a transient hyperpolarization was detectable (Fig. 10*A*), whereas in B6-lpr,lpr no hyperpolarization was observed (Fig. 10*B*). Even though in the rats a causal relationship between NO and superoxide and hyperpolarization could be established, we checked whether in the absence of Fas receptors there was NO and superoxide generation or not. B6 cells showed a large increase in and NO and superoxide in response to 17β-estradiol (Fig. 10, *C* and *D*), whereas in lpr,lpr a comparatively smaller increase in NO and superoxide was noted (Fig. 10, *C* and *D*). Table I shows the death percentages of spermatogenic cells as determined by flow cytometric scanning in both the wild type and the mutant mouse, showing a higher death rate in the spermatogenic cells of B6 mice compared with death in lpr.lpr mice. In summary (i) spermatogenic cells from Fas-deficient mice do not show mitochondrial hyperpolarization in response to 17β-estradiol; (ii) superoxide and NO generation is low in cells from Fas-deficient mice after 17β-estradiol treatment, and estradiol is unable to induce cell death in the absence of Fas.

DISCUSSION

This report illustrates the ability of estradiol to induce apoptosis in different cell types of spermatogenic lineage by direct action in the absence of testicular somatic cells and identifies the participating molecules responsible for cellular apoptosis. Key elements in estradiol-induced changes were an increase in FasL expression; augmented generation of NO, H_2O_2, and superoxide in spermatocytes, spermatids, and spermatogonia; and a transient mitochondrial hyperpolarization resulting in cytochrome *c* release. These changes caused cellular apoptosis, and in the interpretation of the above observations the following questions were addressed: (i) what were the relationships between the above changes? and (ii) how did they translate into apoptotic death?.

The *in vitro* culture of spermatogenic cells was ideal to investigate the direct action of estrogen because early changes induced by estradiol could be measured without the interfer-

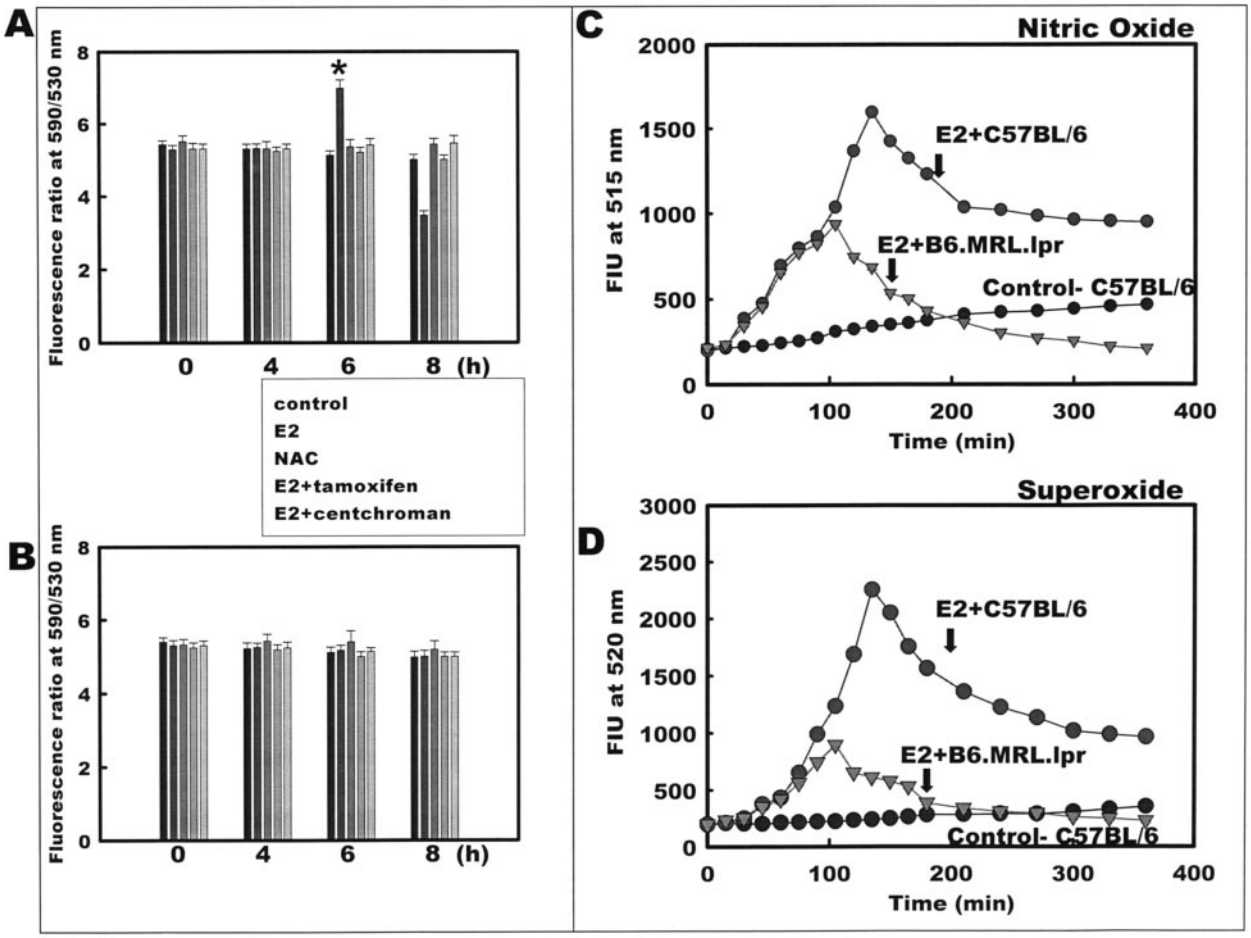

FIG. 10. **17β-Estradiol is unable to induce mitochondrial hyperpolarization in the absence of Fas.** *A* and *B*, effect on mitochondrial membrane polarization. *A*, 17β-estradiol-induced transient hyperpolarization in spermatogenic cells of C57BL/6 mice *in vitro* at 6 h. *B*, 17β-estradiol is unable to induce any change $\Delta\psi_m$ in spermatogenic cells of lpr,lpr mice. $n = 3$, data are mean ± S.E. *, E2 at 6 h *versus* control, $p < 0.05$. *C* and *D*, estradiol effect on NO and superoxide production. *C*, measurement of levels of NO show that although the levels increase in C57BL/6 in response to 17β-estradiol, they did not increase significantly in spermatogenic cells of lpr,lpr mice even after 17β-estradiol exposure, $n = 3$, data are mean ± S.E. *D*, levels of superoxide show that although the levels increase in C57BL/6 in response to 17β-estradiol, they did not increase significantly in spermatogenic cells of lpr,lpr mice even after 17β-estradiol exposure, $n = 3$, data are mean ± S.E.

TABLE I
Effect of estradiol exposure on spermatogenic cell death in C57BL/6 and lpr,lpr mice as recorded from 2 to 8 h after treatment

Groups	2 h	4 h	6 h	8 h
A. C57BL/6 (vehicle-treated)	6.78	8.12	9.41	10.7
B. C57BL/6 (estrogen-treated)	16.50	35.30[a]	43.60[a]	56.4[a]
C. lpr,lpr (vehicle-treated)	5.29	5.45	5.57	5.61
D. lpr,lpr (estrogen-treated)	5.41	5.67	5.73	6.40

[a] B at 4, 6, and 8 h *versus* A at 4, 6, and 8 h and D at 4, 6, and 8 h; $p < 0.05$.

ence of the hypothalamo-hypophyseal axis in this model. The first most significant finding was the recognition of the ability of estradiol to initiate spermatogenic cell death without the help of testicular somatic cell types. Although estradiol receptors α and β are known to be present on spermatogenic cells (41), the consequences of a direct estrogen action on these cells have not been demonstrated. To establish whether the observed estradiol effects were mediated through receptors, tamoxifen was used along with estradiol to investigate whether estradiol-induced changes could be prevented. The presence of tamoxifen reduced cell death, mitochondrial hyperpolarization, FasL up-regulation, and increased ROS and nitrogen species, demonstrating that most of the estradiol-induced changes occurred through hormone-receptor interaction. This observation essentially supports the data that report the presence of estrogen receptors on spermatogonia, pachytene spermatocytes, and round spermatids (41) and to our knowledge demonstrates for the first time that the receptors are functional.

There was clearly a difference in the timing of the type of cells showing DNA fragmentation because pachytene spermatocytes expressed this phenotype earlier than the spermatids. This is possible because pachytene spermatocytes are very susceptible to toxic stimuli, and certain agents have been shown to increase the expression of estrogen receptor β. We observed DNA fragmentation in spermatogonia, although a distinction between type A and B was not possible in the absence of specific markers. A population of diploid cells comprising primarily spermatogonia still survived at 10 h. This could possibly be the result of a longer time required by these cells to enter the apoptotic pathway or a resistance to estradiol.

Various stimuli induce either the extrinsic or the intrinsic apoptotic pathway in the spermatogenic cells (20, 21). This study shows that both the extrinsic pathway involving the cell death receptors and the intrinsic pathway engaging the mitochondria were involved in cell death after estradiol exposure. In many cell types, death receptor stimulation is sufficient to generate caspase activity to complete cell death. However, insufficient caspase activation from death receptor engagement might require further caspase activation from the loss of mitochondrial functions leading to cytochrome *c* release (42). Estrogens are known to activate both types of pathways in several

breast cancer cell lines (42). In this study, evidence of the involvement of cell death receptor pathway came from the observed up-regulation of FasL and the ability of anti-FasL antibody to prevent cell death. Although a FasL increase was evident, Fas increase was not observed, and it appears that the constitutive level was sufficient to initiate the pathway. The detection of soluble FasL in the medium might indicate a possible role of soluble FasL in engaging the Fas receptor. The FasL increase was followed by caspase-8 cleavage, which is the initiator caspase in the death receptor pathway, and Z-LETD-FMK, an inhibitor of the caspase-8, hindered caspase-3 activation. However, Z-LETD-FMK could not interfere with mitochondrial hyperpolarization, showing that the hyperpolarization was dependent on a different set of events.

Mitochondrial dysfunction-initiated cell death leads to cytochrome *c* release from the inner mitochondrial membrane to the cytosol (42). Our observations of the release of cytochrome c preceded by mitochondrial hyperpolarization and the ability of NAC to prevent the mitochondrial dysfunction and cytochrome *c* release suggested that cytochrome *c* release was dependent on mitochondrial membrane dysfunction. Loss of mitochondrial potential is known to occur in many cell types in response to apoptotic stimuli (43), but hyperpolarization is relatively uncommon although it is known to precipitate apoptosis (44). The question at this point was the identity of agents causing mitochondrial disturbances because it could occur as a result of a variety of stimuli including the ROS and nitrogen species. We investigated the generation of ROS and nitrogen species and found that H_2O_2 was not involved in mitochondrial disturbances because NAC was able to reduce hyperpolarization even when H_2O_2 was high. In addition, direct exposure of the spermatogenic cells to H_2O_2 could not induce mitochondrial hyperpolarization. Therefore, it was speculated that either NO or superoxide was creating mitochondrial disturbances. The contribution of NO in hyperpolarization was clear from two observations. First, the presence of AG, an iNOS inhibitor during estradiol treatment, was successful in lowering NO and consequently hyperpolarization. Second, generation of NO using SNAP along with xanthine/xanthine oxidase could induce mitochondrial hyperpolarization, but when SNAP or xanthine/xanthine oxidase was used separately they could not evoke mitochondrial disturbance. Therefore, it was obvious that by themselves both superoxide and NO were unable to initiate mitochondrial damage. The effect of NO could have also been mediated through nitrites to which it is oxidized under physiological conditions or NO could complex with superoxide to form a strong oxidant, peroxynitrite which is a strong cytotoxic agent (45). Although nitrite levels increased in response to estradiol, and it was possible that nitrites or NO could have interacted with mitochondrial components to disrupt its function (46), the ability of MnTBAP, an intracellular peroxinitrite scavenger, to reduce mitochondrial hyperpolarization and cell death effectively essentially showed a peroxynitrite involvement. Interestingly, an increase in NO levels was very pronounced and increased significantly in all three cell populations; however, superoxide did not increase in about 46% of cells. This raises an interesting possibility that the 36% of diploid cells still viable at 10 h could have been saved because NO itself in the absence of superoxide was not sufficient to induce cell death.

Having established that NO and superoxide were the essential components to cause hyperpolarization it was necessary to determine the mechanism of generation of both molecules. Possibilities were that estrogen-induced NO generation increased FasL up-regulation (47) or Fas-FasL ligation resulted in the increase of NO. The inhibition of Fas-FasL ligation by anti-FasL antibodies resulting in the lack of a NO response and reduced NO generation in Fas-deficient cells (lpr,lpr) showed that NO generation was a consequence of Fas-FasL ligation. The inability of NAC to inhibit FasL up-regulation, although it was able to reduce NO and superoxide generation, rules out the involvement of NO and superoxide in FasL increase. Interestingly, although prevention of Fas-FasL binding could reduce NO, it could not inhibit superoxide generation. This was an indication that superoxide generation was not a result of Fas-FasL ligation. The other source of superoxide generation was during the metabolism of estradiol because redox cycling of the semiquinone derivatives of estrogen generate superoxide (27). The observation that ketoconazole, a cytochrome *c* P450 monooxygenase-3A4 inhibitor, prevented the early superoxide production (FIU at 520 nm at 120 min postestradiol; control, 200 ± 18 (3); estradiol, 3,800 ± 300 (3); estradiol + ketoconazole, 190 ± 15 (3)), it strongly suggested metabolism of estradiol as the primary source of superoxide. However, the Fas-deficient cells did not show an increase in superoxide. This contradiction is not explainable because estrogen metabolism was expected to generate superoxide as observed in the rat cells; however, estrogen metabolism might be different in these mutant mice. In the spermatogenic cells, testosterone withdrawal has been shown to induce Fas-FasL ligation (48), and our observations show that another steroid hormone estradiol can also increase FasL expression after 17β-estradiol treatment resulting in the apoptosis of three distinct spermatogenic cell populations: the spermatogonia, spermatocytes, and spermatid.

Therefore in summary, this study establishes the importance of the independent capability of cells of the spermatogenic lineage to respond to estrogens through receptors present on them. Most importantly, the recognition of this ability strongly suggests that low dose estrogens can potentially cause severe spermatogenic cellular dysfunction leading to impaired fertility even without the interference of the hypothalamo-hypophyseal axis.

REFERENCES

1. Korach, K. S. (1994) *Science* **266,** 1524–1527
2. Kuiper, G. G., Enmark, E., Pelto-Huikko, M., Nilsson, S., and Gustafsson, J. A. (1996) *Proc. Natl. Acad. Sci. U. S. A.* **93,** 5925–5930
3. Eddy, E. M., Washburn, T. F., Bunch, D. O., Goulding, E. H., Gladen, B. C., Lubahn, D. B., and Korach, K. S. (1996) *Endocrinology* **137,** 4796–4805
4. Enmark, E., Pelto-Huikko, M., Grandien, K., Lagercrantz, S., Lagercrantz, J., Fried, G., Nordenskjold, M., and Gustafsson, J. A. (1997) *J. Clin. Endocrinol. Metab.* **82,** 4258–4265
5. Hess, R. A. (2003) *Reprod. Biol. Endocrinol.* **1,** 52
6. Toppari, J., and Skakkebaek, N. E. (1998) *Baillieres Clin. Endocrinol. Metab.* **12,** 143–156
7. Sharpe, R. M. (1993) *J. Endocrinol.* **136,** 357–360
8. Colborn, T., vom Saal, F. S., and Soto, A. M. (1993) *Environ. Health Perspect.* **101,** 378–384
9. Nilsson, S., and Gustafsson, J. A. (2002) *Crit. Rev. Biochem. Mol. Biol.* **37,** 1–28
10. Fukuzawa, N. H., Ohsako, S., Nagano, R., Sakaue, M., Baba, T., Aoki, Y., and Tohyama, C. (2003) *Toxicol. in Vitro* **17,** 259–269
11. Atanassova, N., McKinnell, C., Turner, K. J., Walker, M., Fisher, J. S., Morley, M., Millar, M. R., Groome, N. P., and Sharpe, R. M. (2000) *Endocrinology* **141,** 3898–3907
12. Kabuto, H., Amakawa, M., and Shishibori, T. (2004) *Life Sci.* **74,** 2931–2940
13. Akingbemi, B. T., Ge, R., Klinefelter, G. R., Zirkin, B. R., and Hardy, M. P. (2004) *Proc. Natl. Acad. Sci. U. S. A.* **101,** 775–780
14. Iida, H., Maehara, K., Doiguchi, M., Mori, T., and Yamada, F. (2003) *Reprod. Toxicol.* **17,** 457–464
15. Weichselbaum, R. R., Hellman, S., Piro, A. J., Nove, J. J., and Little, J. B. (1978) *Cancer Res.* **38,** 2339–2342
16. Kushner, P. J., Hort, E., Shine, J., Baxter, J. D., and Greene, G. L. (1990) *Mol. Endocrinol.* **4,** 1465–1473
17. Coradini, D., Biffi, A., Pirronello, E., and Di Fronzo, G. (1994) *Anticancer Res.* **14,** 1779–1784
18. Liu, H., Lee, E. S., Gajdos, C., Pearce, S. T., Chen, B., Osipo, C., Loweth, J., McKian, K., De Los, R. A., Wing, L., and Jordan, V. C. (2003) *J. Natl. Cancer Inst.* **95,** 1586–1597
19. Song, R. X., and Santen, R. J. (2003) *Apoptosis* **8,** 55–60
20. Sinha Hikim, A. P., Lue, Y., Diaz-Romero, M., Yen, P. H., Wang, C., and Swerdloff, R. S. (2003) *J. Steroid Biochem. Mol. Biol.* **85,** 175–182
21. Print, C. G., and Loveland, K. L. (2000) *Bioessays* **22,** 423–430
22. Nair, R., and Shaha, C. (2003) *J. Biol. Chem.* **278,** 6470–6481

23. D'Alessio, A., Riccioli, A., Lauretti, P., Padula, F., Muciaccia, B., De Cesaris, P., Filippini, A., Nagata, S., and Ziparo, E. (2001) *Proc. Natl. Acad. Sci. U. S. A.* **98,** 3316–3321
24. Sapi, E., Brown, W. D., Aschkenazi, S., Lim, C., Munoz, A., Kacinski, B. M., Rutherford, T., and Mor, G. (2002) *J. Soc. Gynecol. Investig.* **9,** 243–250
25. Mor, G., Sapi, E., Abrahams, V. M., Rutherford, T., Song, J., Hao, X. Y., Muzaffar, S., and Kohen, F. (2003) *J. Immunol.* **170,** 114–122
26. Koji, T., and Hishikawa, Y. (2003) *Arch. Histol. Cytol.* **66,** 1–16
27. Farinati, F., Cardin, R., Bortolami, M., Grottola, A., Manno, M., Colantoni, A., and Villa, E. (2002) *Mol. Cell. Endocrinol.* **193,** 85–88
28. Djavaheri-Mergny, M., Wietzerbin, J., and Besancon, F. (2003) *Oncogene* **22,** 2558–2567
29. Devadas, S., Hinshaw, J. A., Zaritskaya, L., and Williams, M. S. (2003) *Free Radic. Biol. Med.* **35,** 648–661
30. Perez-Cruz, I., Carcamo, J. M., and Golde, D. W. (2003) *Blood* **102,** 336–343
31. Denning, T. L., Takaishi, H., Crowe, S. E., Boldogh, I., Jevnikar, A., and Ernst, P. B. (2002) *Free Radic. Biol. Med.* **33,** 1641–1650
32. Meistrich, M. L., Longtin, J., Brock, W. A., Grimes, S. R., Jr., and Mace, M. L. (1981) *Biol. Reprod.* **25,** 1065–1077
33. Rao, A. V., and Shaha, C. (2000) *Free Radic. Biol. Med.* **29,** 1015–1027
34. Dey, R., and Moraes, C. T. (2000) *J. Biol. Chem.* **275,** 7087–7094
35. Duranteau, J., Chandel, N. S., Kulisz, A., Shao, Z., and Schumacker, P. T. (1998) *J. Biol. Chem.* **273,** 11619–11624
36. Aravinda, S., Gopalakrishnan, B., Dey, C. S., Totey, S. M., Pawshe, C. H., Salunke, D., Kaur, K., and Shaha, C. (1995) *J. Biol. Chem.* **270,** 15675–15685
37. Johnson, L., Neaves, W. B., Barnard, J. J., Keillor, G. E., Brown, S. W., and Yanagimachi, R. (1999) *Biol. Reprod.* **61,** 927–934
38. Kaufmann, S. H., and Hengartner, M. O. (2001) *Trends Cell Biol.* **11,** 526–534
39. Knox, P. G., Milner, A. E., Green, N. K., Eliopoulos, A. G., and Young, L. S. (2003) *J. Immunol.* **170,** 677–685
40. You, H. J., Kim, J. Y., and Jeong, H. G. (2003) *Biochem. Biophys. Res. Commun.* **303,** 1129–1134
41. O'Donnell, L., Robertson, K. M., Jones, M. E., and Simpson, E. R. (2001) *Endocr. Rev.* **22,** 289–318
42. Ohta, S. (2003) *Curr. Med. Chem.* **10,** 2485–2494
43. Ly, J. D., Grubb, D. R., and Lawen, A. (2003) *Apoptosis* **8,** 115–128
44. Liang, B. C., Miller, L., and Weller, A. (1999) *Apoptosis* **4,** 89–97
45. Kang, Y. C., Kim, P. K., Choi, B. M., Chung, H. T., Ha, K. S., Kwon, Y. G., and Kim, Y. M. (2004) *In Vivo* **18,** 367–376
46. Radi, R., Cassina, A., Hodara, R., Quijano, C., and Castro, L. (2002) *Free Radic. Biol. Med.* **33,** 1451–1464
47. Amant, C., Holm, P., Xu Sh, S. H., Tritman, N., Kearney, M., and Losordo, D. W. (2001) *Circulation* **104,** 2576–2581
48. Nandi, S., Banerjee, P. P., and Zirkin, B. R. (1999) *Biol. Reprod.* **61,** 70–75

Molecular Basis of Cell and Developmental Biology:

Estrogen-induced Spermatogenic Cell Apoptosis Occurs via the Mitochondrial Pathway: ROLE OF SUPEROXIDE AND NITRIC OXIDE

Durga Prasad Mishra and Chandrima Shaha

J. Biol. Chem. 2005, 280:6181-6196.
doi: 10.1074/jbc.M405970200 originally published online November 15, 2004